Aus der Klinik für Nuklearmedizin
der Medizinischen Fakultät Charité – Universitätsmedizin Berlin

DISSERTATION

Role of MRI and FDG-PET in the exploration of the Entorhinal Cortex in relation to spatial orientation in patients with mild cognitive impairment

Bedeutung der MRT und FDG-PET in der Exploration des Entorhinalen Kortex in Zusammenhang mit der räumlichen Orientierung bei Patienten mit leichter kognitiver Beeinträchtigung

zur Erlangung des akademischen Grades
Doctor medicinae (Dr. med.)

vorgelegt der Medizinischen Fakultät
Charité – Universitätsmedizin Berlin

von

Asma Hallab

Datum der Promotion: 25.11.2022

I- Table of contents

This dissertation is based on my following Publication:

Hallab, A., Lange, C., Apostolova, I., Özden, C., Gonzalez-Escamilla, G., Klutmann, S., Brenner, W., Grothe, M. J., Buchert, R., & Alzheimer's Disease Neuroimaging Initiative (2020). Impairment of Everyday Spatial Navigation Abilities in Mild Cognitive Impairment Is Weakly Associated with Reduced Grey Matter Volume in the Medial Part of the Entorhinal Cortex. Journal of Alzheimer's disease : JAD, 78(3), 1149–1159. (1)

II- List of abbreviations

AD: Alzheimer’s disease

ADAS13: Alzheimer’s Disease Assessment Score (ADAS-Cog-13)

ADNI: Alzheimer's Disease Neuroimaging Initiative

BA: Brodmann Areas

BA 28: Brodmann Area 28

BA 34: Brodmann Area 34

ECog: Everyday Cognition

ERC: Entorhinal Cortex

FDG-PET: Fluorodeoxyglucose Positron Emission Tomography

FDGu: Fluorodeoxyglucose Uptake

fMRI: Functional Magnetic Resonance Imaging

GC: Grid Cells

GMV: Grey Matter Volume

LEC: Lateral Entorhinal Cortex

MRI: Magnetic Resonance Imaging

MCI: Mild Cognitive Impairment

MEC: Medial Entorhinal Cortex

MNI: Montreal Neurological Institute

MMSE: Mini-Mental State Examination

PHC: Parahippocampal Cortex

PRC: Perirhinal Cortex

PVE: Partial Volume Effect

VISSPAT: Visuospatial Ability Scores of the Everyday Cognition Test

III- Abstract in English

Background: The entorhinal cortex (ERC) has become a center of growing interest since the description of ERC neurons especially encoding for spatial navigation and spatial memory. In rodents, those cells are particularly found in the medial side of the ERC. Studies in humans are limited, in particular there is no study clearly identifying the homolog of the rodent medial ERC in humans so far.

Objective: Brodmann areas (BA) 34 and 28 are major components of the ERC in humans. The aim of this study was to evaluate whether BA 34 or BA 28 might be considered the homolog to the medial ERC in rodents with respect to spatial navigation abilities, and to evaluate the role of MRI and FDG-PET in the exploration of both regions in relation to spatial orientation in patients with mild cognitive impairment (MCI).

Methods: Patients with MCI from the Alzheimer's Disease Neuroimaging Initiative (ADNI) were included if they had the entire visuospatial (VISSPAT) ability scores of the Everyday Cognition (ECog) test as well as high-resolution T1-weighted MRI and brain FDG-PET performed within 30 days of the ECog test. Grey matter volume and FDG uptake in each of ERC Brodmann areas (BA 34 and BA 28) were calculated from MRI and FDG-PET using predefined standard masks of BA 34 and BA 28. Regression and multivariate analyses of covariance were employed for statistical analyses.

Results: The eligibility criteria were fulfilled by 379 MCI patients. Amongst all studied subdomains assessed by the ECog test, only spatial navigation performance, as characterized by the self-reported VISSPAT sum score, was

correlated with the integrity of BA 34 (grey matter volume but not FDG uptake). None of the ECog subscores was correlated with BA 28 integrity (neither grey matter volume nor FDG uptake).

Conclusion: Impairment of orientation skills and spatial memory in MCI is more strongly associated with atrophy of BA 34 compared to BA 28, suggesting that BA 34 rather than BA 28 is the human homolog of the rodent medial ERC with respect to spatial orientation abilities. Spatial orientation performance was not associated with glucose metabolism in BA 34, presumably due to higher between-subjects variability of (partial volume-corrected) FDG uptake in BA 34 used to characterize its glucose metabolism.

IV- Abstract in German

Hintergrund: Der entorhinale Kortex (ERC) ist seit der Beschreibung von ERC-Neuronen, die insbesondere für die räumliche Navigation und das räumliche Gedächtnis kodieren, von zunehmenden Interesse. Bei Nagetieren befinden sich diese Zellen insbesondere im medialen Teil des ERC. Studien am Menschen sind begrenzt, insbesondere gibt es bisher keine Studie, die das Homolog des medialen ERC von Nagern beim Menschen eindeutig identifiziert.

Ziel: Die Brodmann-Areale (BA) 34 und 28 sind wesentliche Bestandteile des ERC bei Menschen. Das Ziel dieser Studie war es zu testen, ob BA 34 oder BA 28 in Bezug auf die räumlichen Navigationsfähigkeiten als Homolog des medialen ERC bei Nagetieren angesehen werden können, und die Bedeutung der MRT und FDG-PET für die Exploration der beiden Hirnareale bei Patienten mit leichter kognitiver Beeinträchtigung zu evaluieren.

Methoden: Patienten mit leichter kognitiver Beeinträchtigung aus der Alzheimer's Disease Neuroimaging Initiative (ADNI) wurden eingeschlossen, wenn sie einen vollständigen visuellen (VISSPAT) Fähigkeitsscore des Everyday Cognition (ECog)-Tests sowie hochauflösende T1-gewichtete MRT und FDG-PET Bilder des Gehirns aufwiesen, die innerhalb von 30 Tagen nach dem ECog-Test erstellt wurden. Das Volumen der grauen Substanz und die FDG-Aufnahme in BA 34 und BA 28 wurden aus MRT und FDG-PET Bildern unter Verwendung vordefinierter Standardmasken von BA 34 und BA 28 berechnet. Für die statistische Analyse wurden Regressions- und multivariate Kovarianzanalysen eingesetzt.

Ergebnisse: Die Auswahlkriterien wurden von 379 MCI-Patienten erfüllt. Von allen durch den ECog-Test bewerteten Subdomänen korrelierte nur die räumliche Navigationsleistung aus dem selbst berichteten VISSPAT-Summenscore mit der Integrität von BA 34 (Volumen der grauen Hirnsubstanz, aber nicht FDG-Aufnahme). Keiner der ECog-Subscores war mit der BA 28-Integrität korreliert (weder das Volumen der grauen Substanz noch die FDG-Aufnahme).

Schlussfolgerung: Die Beeinträchtigung der Orientierungsfähigkeit und des räumlichen Gedächtnisses bei MCI ist stärker mit einer Atrophie von BA 34 im Vergleich zu BA 28 verbunden, was darauf hindeutet, dass BA 34 und nicht BA 28 das menschliche Homolog des medialen ERC von Nagetieren in Bezug auf räumliche Navigationsfähigkeiten ist. Die räumliche Navigationsleistung war nicht mit dem Glukosestoffwechsel in BA 34 korreliert, vermutlich aufgrund der höheren Variabilität der (teilweise volumenkorrigierten) FDG-Aufnahme in BA 34, die zur Charakterisierung des Glukosestoffwechsels verwendet wurde.

V- Cover text

The current doctoral research is a neuroscience project, performed in the Department of Nuclear Medicine, Charité – Universitätsmedizin Berlin, and based on a specific topic covering the spatial orientation in MCI patients, brain morphology, and molecular imaging.

The region of interest of this work is the Entorhinal cortex (ERC), which has been so far less studied than other brain structures of the medial temporal lobe. Since the description of its various cells, mainly playing a role in defining and organizing the spatial orientation, the ERC has attracted rising scientific interest aiming to better understand its morphology and function. Spatial cells were first identified and described mainly in the medial ERC in rodents. Later, based on single neuron coding and functional MRI (fMRI), evidence of similar findings has been reported in humans. Thus there was, to date of designing this study, no morphological or metabolic studies exploring the ERC in relation to spatial orientation and defining the predictive value of MRI and FDG-PET in everyday practice.

1. Entorhinal cortex

The ERC has been recognized as the main brain region defining the spatial orientation and navigation skills in rodents and humans. Various cells, firing based on computational models and correlated to a specific function in relation to spatial navigation, have been described in ERC.

1.1. Anatomy

The ERC is located in the medial temporal lobe and corresponds mainly to BA 28 (2) (known as “area entorhinalis” or “ventral” ERC (3)) and BA 34 (known as “area entorhinalis dorsalis”), and it is described by some authors as the “cortico-medial part of the amygdaloid complex”. (4) Brodmann described both areas separately since they have distinct properties and connectivities. (5) (Figures 1 and 2)

It has been reported in animals and particularly in rodents, that the medial ERC mainly supports the spatial orientation, (6, 7) while the lateral ERC supports the temporal orientation, (8) and the olfactory and sensory information. (9, 10)

ERC plays the role of junction between the hippocampus on the one side, and different cortex areas on the other side. Each part of the ERC have projections to various hippocampal structures (subiculum, CA3, CA2, CA1 fields, and dentate gyrus). (2)

In rodents, the medial ERC processes spatial information through inputs from parahippocampal cortex (PHC), while the lateral ERC gets item-related information from perirhinal cortex (PRC). The hippocampus receives cortical input from those two major pathways. (11)

In order to bridge the gap in observations and studies between rodents and humans, researchers used 7 Tesla fMRI in humans and showed that the ERC is functionally divided from front-to-back. The lateral ERC (LEC) in rodents corresponds to the anterior-connected ERC in humans and the medial ERC (MEC) in rodents corresponds to posterior-connected ERC in humans. (12) In humans, similar functional roles of the parahippocampal cortex and perirhinal cortex have been described. (13, 14)

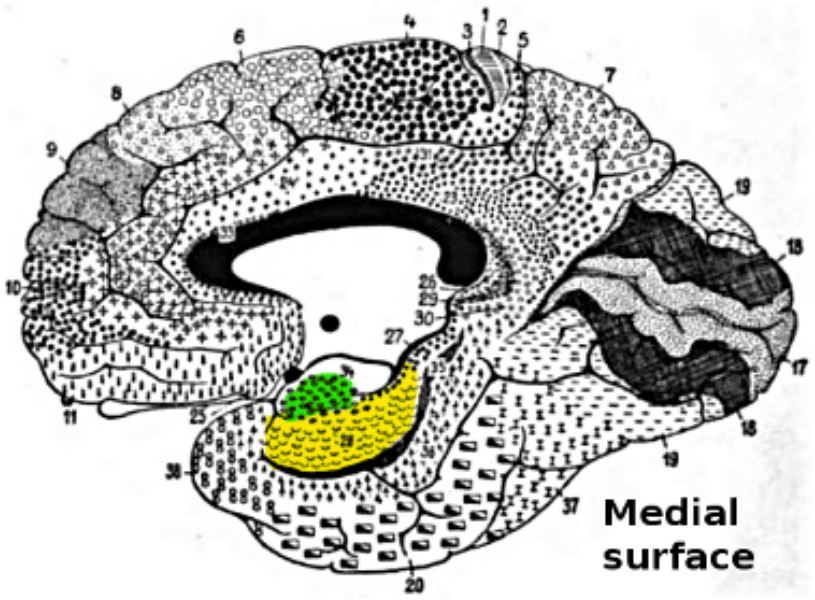

Figure 1: Location of Brodmann Areas 34 (green) and 28 (yellow) in the medial temporal lobe. (From Brodmann's cytotechtonic map (1909), published by Wikipedia, with modification) (15, 16)

Figure 2: Brain dissection showing the Entorhinal cortex (ERC) in the medial temporal lobe in relation to the hippocampus and adjascent structures. (Own picture taken during Neuroanatomy course in LMU – 2019, after the friendly authorization from the course supervisors).

ERC spatial cells in primates:

For a better overview on the anatomical structures which play a role in the spatial orientation, different neurons with a particular spatial orientation functionality are described in the following part. Those are, among others: place cells, head direction cells, boundary (or border) cells, grid cells, object-encoding cells, and object-vector cells.

1.1.1. Place cells

Place cells were first described in 1971 by O'Keefe and Dostrovsky in the hippocampus of a freely behaving rat. (17) Those cells show a topography-graded variation in their firing aspects; the signal recorded at the ventral sites of the hippocampus tend to have larger fields than at dorsal sites. (18) Consequently, they allow the animal recognizing its environment based on different scales. (18) Although place cells show correlations between their activity and spatial variables, their function is also sensitive to modifications in other environmental aspects (exp. odor or color). (19) Such nongeometric information help discriminating various subsets in spatial contexts.

1.1.2. Head direction cells

Head direction cells were first described in 1990 by Taube and his collaborators in the postsubiculum, (20) but were later also recorded in MEC. (7) Various following studies have shown that head direction cells are located in different cerebral regions, and that their function is based on vestibular, motor and proprioceptive information. (21) Each of those cells has a unique preferred direction; its firing potential is at his maximum level when the animal is facing in

the corresponding specific direction and decreases when the head direction changes to the different side. (20)

1.1.3. Grid cells

Grid Cells (GC) were first described in 2005 by Moser and collaborators (6) in the MEC of rodents, but later also in the pre- and parasubiculum. (22) The particularity of the GC is the ability of each of firing in multiple fields and the tessellation of the environment with a hexagonal grid formation. (23) Three properties characterize the GC: scale, orientation, and size (of the field). (6) Those three periodic components are of similar wavelength (scale) and oriented on 60° intervals; the 60° rotation symmetry of GC is one of their main characteristics. (6) Moreover, when the rodent is located in a new environment, grids show changes in their structures (which become less regular) and in their scales (which expand). As soon as the environment becomes familiar, the grids regain their habitual scale and regularity. (24) Further studies showed that GC have a definite scale independent from the body size of the rodent. (25)

1.1.4. Boundary cells

Boundary cells were described in subiculum, (26) presubiculum and parasubiculum (22) and in MEC (27) and might have different properties. Stewart and collaborators reported, for example, that “boundary-vector” cells in the subiculum respond similarly to different environmental boundaries independently of their different properties (drop edges versus walls). (28) Such information support the cognitive mapping of the spatial environment.

1.1.5. Object-encoding cells

Object-encoding cells are mainly located in LEC, and they fire when the animal reaches a specific known object in a particular location. (29) They mainly provide information about a specific component of the spatial environment and ensure an object-place memory in interaction with the hippocampus. (11, 29)

1.1.6. Object-vector cells

Described in 2019 by Moser and collaborators, object-vector cells are located in the superficial layers of MEC and encode, independently from objects' locations, seizes and identities, the distance and direction that separates them. Experiments showed a strong interconnection between object-vector cells and the network of GC and head direction cells. (30) These cells promote the allocentric (individual-independent) orientation in the environment.

1.1.7. Goal-vector hippocampal cells

Compared to their entorhinal counterparts, who respond to every single object, goal-vector cells in CA1 respond only to specific goals. They ensure a goal-directed navigation, which promotes the egocentric orientation in the space, and are memory-based. (31) Moreover, the hippocampal cells respond to each object at a specific location, and they are considerably affected when goals are displaced. (30) A training effect of entorhinal cells toward hippocampal cells might explain the differences between both entities and the memory-based aspect of the latter. (32)

1.2. Role of Entorhinal cortex in human subjects

In previous rodent works, hippocampal, medical temporal cells and medial prefrontal cells showed phase-coding related to theta oscillation during navigation. In human electrophysiological studies, phase-coding in medial temporal neurons appeared to be related to navigational planning and goal arrival, too. (33) Combining the results of single-unit electrophysiology and fMRI in human subjects, signals indicating the firing of GC were observed in different brain regions (exp. Subicular, entorhinal, posterior and medial parietal areas, as well as the lateral temporal and medial prefrontal areas). Thus, the strongest signal was registered in the right ERC. (34)

The medial-projected part of ERC contains cells processing the spatial navigation such as GC and receives its inputs from PHC. The lateral-projected part of ERC contains cells processing objects and receives its inputs from PRC. Like already described in animal models, both of those ERC parts integrate multimodal spatial and sensory information from the cortex and give outputs to the hippocampus. Through its complex processing system, the ERC contributes to the generation of spatial memory or a cognitive map in the hippocampal cells. (12, 35)

In addition to natural vestibular and proprioceptive signals, which influence navigation in real space, visual information play a central role in the active and virtual navigation and modulate GC in ERC in both situations.

Nadasdy and collaborators reported in human subjects, and in contrary to rodents, a more rapid adaptation of GC to environmental entities and structures, which suggests an active and instantaneous GC-based spatial encoding in humans. The visual inputs might play a more central and efficient role in the

orientation and navigation process in humans compared to rodents, which proves the complexity of the spatial navigation in humans on one side, but also might help explaining the ability of a much more rapid mapping of spatial information, on the other side. (36)

Moreover, recent studies in humans showed that there is a lateralization of brain functions in term of spatial orientation and that the right temporo-parietal cortex in right-handers is dominant in processing the spatial navigation and in the elaboration of the spatial memory. (37)

Understanding the neural representation and functioning of spatial memory might help better understand further cognitive aspects in human subjects, which might be based on a grid-like pattern, as well. (38)

1.3. Alzheimer's disease and Entorhinal cortex:

ERC is one of the initial cerebral regions affected by neurodegeneration during the Alzheimer's disease (AD) process. (39) Some studies related its dysfunction to an accumulation of plaques, tangles and Tau protein, which leads to a reduced synaptic plasticity and progressive cell death and results in spatial desorientation and impaired cognition. The impairment of neurons and neurotransmitters in the MEC occurs months before memory alteration. (40)

The hippocampus has attracted much interest during the last 20 years owing to its role in memory and as one of the anatomical structures early affected during AD. (41, 42) Nevertheless, due to its complexity, ERC has been less explored and some recent studies showed that this structure is even earlier affected than the hippocampus by the degenerative process related to AD. (43, 44)

The extended aging process related to the improvement of health care standards led to a rapid growth in dementia's incidence during the last few decades. (45) According to the World Health Organization, AD is the most common cause of the dementia syndrome (60-70%) and affects a high proportion of the global population, turning it to the center of big scientific interest in view of its significant impact on health costs. (46) Subjects with mild cognitive impairment (MCI), a lower form of cognitive decline than dementia, are at risk of developing AD. (47) The definition and markers of MCI have been evolving constantly and are attracting widespread attention. In this context, Alzheimer's Disease Neuroimaging Initiative (ADNI), a non-randomized longitudinal observational study, was launched in 2004 and aims to understand the process of brain aging and evolution from MCI to AD. Enrolled subjects are mainly from the USA and Canada, and they are either of normal cognition, MCI, or early AD individuals. (48) Due to the absence of a curative treatment for neurodegeneration leading to dementia, there is a growing interest to identify early clinical and radiological markers predicting prodromal stages of cognitive decline and in proposing early interventions to slow down the progression to dementia.

2. Aims

The approach used in this work aimed to investigate ADNI-results based on volumetric brain analyses through structural magnetic resonance imaging (MRI), on one side, and evaluation of glucose metabolism based on positron emission tomography (PET), on the other side. The ^{18}F-fluoro-deoxy-glucose (FDG), a glucose analog, was used as marker for neuronal activity. The purpose of this study was to analyze MCI patients with and without impairment of spatial orientation and to evaluate whether there are any structural and metabolic changes corresponding to ERC which could potentially highlight its role in spatial orientation and navigation during MCI.

The current study aimed to test the following hypotheses: first, whether spatial navigation performance and spatial memory, as suggested by the visuospatial domain of everyday cognition test (VISSPAT), are specifically correlated with the grey matter volume (GMV) in BA 34 (rather than in BA 28). Second; whether partial volume corrected FDG uptake (FDGu), specifically in BA 34, could be a significant predictor for spatial navigation performance and spatial memory in MCI patients independently of GMV. (1)

3. Note

In this publication-based dissertation the same database and consequently the same included MCI-patients, as reported in the manuscript, (1) were included. This led to similarities in some parts of the dissertation with the published manuscript. For example, the description of the selection strategy in the results part, which is, in this dissertation, better highlighted using a chart flow. The methods used to gain the neuroimaging data were also previously described in the manuscript. (1)

In order to extend the methods used in the exploration of the study aims, I am reporting here supplementary data and statistic strategies, which makes the dissertation broader and complementary to the manuscript. For example, the description of the included population is more detailed in the following results part. Additionally, to further evaluate the findings based on self-reported VISSPAT tests, I compared them with findings based on study partner-reported (SP-VISSPAT) results in relation to the regions of interest (BA 34 and BA 28) and using both neuroimaging methods. Further, I compared other aspects from ECog test, such as language and memory, with the findings of the visuospatial orientation (VISSPAT), also in relation to the regions of interest (BA 34 and BA 28) based on both neuroimaging methods.

Differently from the manuscript, where “dichotomized” VISSPAT sum score was used for the multivariate analysis, (1) here I used the “continuous” value of VISSPAT sum score for the multivariate and univariate analyses in all its steps, independently from the cut-off value, that was used in the manuscript in order to define the navigation performance (“impaired” vs. “preserved”). Moreover, I

compared the multivariate and univariate analyses of “continuous” VISSPAT with those of “continuous” SP-VISSPAT sum score.

4. Methods

Some parts of the subsequent methods and strategies have been published in the manuscript. (1)

4.1. Population: ADNI Study

ADNI is a non-randomized longitudinal natural history study. Participants have been mainly enrolled in 63 sites in the USA and Canada. The overall aim of the ADNI study was to validate specific biomarkers (biological parameters, MRI, PET, clinical and neuropsychiatric assessments) in order to evaluate the risk of progression from MCI to AD and for use in clinical trials related to AD's treatment. ADNI, led by Michael W. Weiner, MD (principal investigator), has been running since 2004 and was initially funded until 2021. To date over 2000 scientific publications have been shared based on ADNI data, which is available embargo-free to researchers worldwide. There are currently 4 phases in ADNI studies: ADNI 1, ADNI Go, ADNI 2, and ADNI 3. In each phase, more participants have been enrolled, and more developed investigations have been used. (48)

Following details about the study population were reported from the main website of ADNI (http://adni.loni.usc.edu/): (48)

ADNI enrolled participants between the ages of 55 and 90 years. After informed consent, participants are monitored regularly through neuropsychological tests over the next consecutive years. **Inclusion criteria** were: non-pathological scores in the geriatric depression scale test, available partner with a regular contact with the study participant, adequate visual and auditory aptitude, good

general health, motivation for taking the tests and for undergoing the neuroimaging investigations, fluency in English or Spanish, and the participant must have accomplished six grades of education or have a good work history (in order to exclude mental retardation). **Exclusion criteria** were mainly: evidence of infection or cerebro-vascular disease at MRI, contra-indications for undergoing MRI or FDG-PET scanning, a major-depression episode or a positive history of other psychiatric disorders or alcohol abuse, unstable medical conditions, or abnormalities in Vitamin B12 and Folate or their correlated markers' levels, and psychoactive medication. (48)

Inclusion criteria for MCI in ADNI study

In order to be diagnosed with MCI, participants should present a subjective memory concern. This might be reported by the participant itself, his partner, or the clinician. Furthermore, the MMSE score should be between 24 and 30. The Clinical Demential Rating must be at least 0,5. Impaired memory function should be also documented by scoring within the education adjusted ranges on the Logical Memory II subscale (Delayed Paragraph Recall, Paragraph A only) from the Wechsler Memory Scale, revised. AD should be excluded by proving that the general cognition and functional performance are sufficient. Finally, the permitted medication should be stable for the last four weeks. (48)

MCI patients

For the purpose of the actual study, the baseline data of 458 ADNI MCI subjects with the visuospatial domain of ECog, MRI (MPRAGE), and cerebral FDG-PET was downloaded from ADNI repository (http://adni.loni.usc.edu/). (48) The baseline population, as also reported in the manuscript, had a mean age of 71.70±7.40 years and females represented 45.2% of the sample. The APOE4 profile was positive in 47.8% of cases. (1)

4.2. Cognitive assessment: Everyday cognition

ECog is a measure of cognitively-relevant everyday abilities; it could either be reported by the patient itself (self-reported) or by a second person who has a close contact with the patient (study-partner). It is composed of 39 different items and covers six cognitively-relevant domains: “Everyday Memory, Everyday Language, Everyday Visuospatial Abilities, and Everyday Planning, Everyday Organization, and Everyday Divided Attention”. (49)

The rating is based on a 4-point scale and scores aim for each item to evaluate the current level of daily functioning in contrast with the functioning ability 10 years earlier:

“1 = better or no change compared to 10 years earlier”,

“2 = questionable/occasionally worse”,

“3 = consistently a little worse”,

“4 = consistently much worse”.

4.2.1. Everyday visuospatial abilities: Self-reported

In the present study, spatial orientation performance was evaluated by a VISSPAT sum score obtained through summation of the seven subscores, then subtracting seven: “following a map to find a new location” (VISSPAT 1), “reading a map and helping with directions when someone else is driving” (VISSPAT 2), “finding my car in a parking lot” (VISSPAT 3), “finding my way back to a meeting spot in the mall or other location” (VISSPAT 4), “finding my way around a familiar neighborhood” (VISSPAT 6), “finding my way around a familiar store” (VISSPAT 7), and “finding my way around a house visited many times” (VISSPAT 8). In the current investigation, VISSPAT 5, a duplicate score, was omitted. The VISSPAT sum score was detailed in the manuscript and ranged between 0 and 21 (0: “intact”, 21: “severely impaired”). (1)

4.2.2. Everyday visuospatial abilities: Reported by study partner

In order to compare findings related to spatial navigation reported by patients themselves and those reported by their partners, I followed the same strategy with the same subscores collected from the study partners: “following a map to find a new location” (SP-VISSPAT 1), “reading a map and helping with directions when someone else is driving” (SP-VISSPAT 2), “finding my car in a parking lot” (SP-VISSPAT 3), “finding my way back to a meeting spot in the mall or other location” (SP-VISSPAT 4), “finding my way around a familiar neighborhood” (SP-VISSPAT 6), “finding my way around a familiar store” (SP-VISSPAT 7), and “finding my way around a house visited many times” (SP-VISSPAT 8). In the current investigation, SP-VISSPAT 5 was omitted for the same previous reason. For this strategy, I omitted, at a second stage, SP-

VISSPAT 1 and SP-VISSPAT 2 because they are mainly based on language and communication, in order to avoid the bias presented by those subscores. The SP-VISSPAT (3-8) sum score ranged between 0 and 15 (0: “intact”, 15: “severely impaired”). At this stage, in order to compare data, I followed the same strategy to calculate VISSPAT (3-8) sum score.

4.2.3. Everyday memory: Self-reported

I followed the same strategy with the ECog domain related to memory and obtained a MEMORY sum score by adding the following eight subscores then subtracting eight: “remembering a few shopping items without a list” (MEMORY 1), “remembering things that happened recently” (MEMORY 2), “recalling conversations a few days later” (MEMORY 3), “remembering where I have placed objects” (MEMORY 4), “repeating stories and/or questions” (MEMORY 5), “remembering the current date or day of the week” (MEMORY 6), “remembering I have told someone something” (MEMORY 7), and “remembering appointments, meetings, or engagements” (MEMORY 8). Patients with at least a single score of 9 (who gave no answer to at least one question) were dropped out. The MEMORY sum score ranged between 0 and 24 (0: “intact”, 24: “severely impaired”).

4.2.4. Everyday language: Self-reported

Further, I followed the same strategy with the ECog domain related to language and obtained a LANGUAGE sum score through adding the following nine subscores then subtracting nine: “forgetting the names of objects” (LANG 1), “verbally giving instructions to others” (LANG 2), “finding the right words to use

in conversations" (LANG 3), "communicating thoughts in a conversation" (LANG 4), "following a story in a book or TV" (LANG 5), "understanding the point of what other people are trying to say" (LANG 6), "remembering the meaning of common words" (LANG 7), "describing a program I have watched on TV" (LANG 8), "understanding spoken directions or instructions" (LANG 9). Patients with at least a single score of 9 (who gave no answer to at least one question) were dropped out. The LANGUAGE sum score ranged between 0 and 27 (0: "intact", 27: "severely impaired").

Cases with no longer than 30 days-delay separating the molecular imaging (FDG-PET) and the neuropsychological testing (ECog) were included in the current study. For longer delays between both investigations, patients were considered non-eligible and were excluded. (1)

4.3. BA 34 and BA 28 FDG uptake

Following steps of glucose metabolism measurement based on FDGu in both BA regions were also described in the manuscript. (1)

Owing to the multicentricity of ADNI and the various protocols followed for the PET scan acquisition, some differences were reported in the methods used. In fact, the acquisition started thirty minutes after injection, but data was acquired either as a single static scan of thirty minutes span, or as thirty-three frames of one minute span, or as six frames of five minutes span. The reconstruction of the images was performed with a local software. Yet, in order to harmonize the data quality from different sources, settings were unified. (1) Different PET procedure manuals could be downloaded from the following ADNI address:

https://adni.loni.usc.edu/wp-content/uploads/2010/09/PET-Tech_Procedures_Manual_v9.5.pdf.

For the originality of the data, images were downloaded in following formats ("as archived", "ECAT", "Interfile", or "DICOM"), and were converted to "Nifti file format". Therefore, "SPM8" was applied for "ECAT" and "DICOM" files, while "ImageConverter" (v. 1.1.5) was used for "Interfile" files. (1)

In case of a "dynamic" acquisition of the PET scan, SPM8-Realign-Tool was applied in order to detect the interframe motion. The initial frame was considered the "reference". By trailing then inside the cerebral area five different references, the estimation of the degree of motion of the following frames in relation to the initial one was possible. (50) A motion degree over 4 mm led to the elimination of the corresponding frame. (51) After aggregating all remaining frames, a motion-free PET image was achieved. (50) The coregistration of MRI and PET images was performed by SPM8. (1)

"FDG uptake" values reported in this current study, referrer permanently to "mean PVE-corrected FDG uptake scaled to mean non-PVE-corrected FDG uptake in the pons", with PVE referring to partial volume effect. (1) This MRI-dependent PVE adjustment, was obtained referring to the Müller-Gärtner technic as integrated in the SPM toolbox ("PETPVE12"). (52) Average PVE-corrected BA 34 and BA 28 FDGu were scaled to the average of non-PVE-adjusted FDGu of pons-area. (53) That led to the exclusion of cases, where the PET scans did not include axially the pons in its totality. (1)

4.4. BA 34 and BA 28 Grey matter volumes

Following steps of measurement of GMV in both BA regions were described in the manuscript. (1)

For the identification of the region of interests needed for this study and based specifically on the Brodmann areas, the Pickatlas-tool from the Wake Forest University School of Medicine (53, 54) was used. Both regions, BA 34 and BA 28, presented binary masks bilaterally and were predetermined in the anatomical space of Montreal Neurological Institute (MNI). (1)

In order to obtain personalized and definite maps of probability corresponding to cerebrospinal fluid, GMV, and white matter volume, a method based on a unified segmentation was followed to perform the segmentation of MRI data of included patients. (54) This technic is integrated in the statistical parametric mapping software package - SPM12 (Wellcome trust center for neuroimaging, London, UK). With the exception that the graphical material had to be converted to a 2mm-sample, all other settings were kept unchanged. (55) Then, the BA 34 and BA 28 binary masks were converted into specific patient space, as suggested by the unified segmentation. (1)

BA 34 and BA 28 GMV were calculated as following: first, a voxel-based multiplication of the transformed BA mask with the grey matter probability map, as suggested by the SPM segmentation, was performed. Then, all voxel values were summed. Finally, the sum was multiplied by the single-voxel volume. In this procedure, no threshold for a grey matter probability was implemented. (1)

4.5. Statistical analyses

Mean values of BA 34 GMV, BA 34 FDGu, BA 28 GMV, and BA 28 FDGu were measured. Same as in the manuscript, cases were considered “outliers” if they presented a value exceeding three standard deviations from the corresponding mean. For a higher specificity of the data, those cases were then removed. Moreover, to suppress the risk of an over-corrected PVE, a difference superior to three standard deviations in the mean FDGu between both cases (PVE correction vs. no PVE correction), either in BA 34 or BA 28, was an exclusion criteria. (1) For a broader and detailed description of the neuroimaging findings based on each VISSPAT subscore and value, I performed a comparison of means using t-test and visualized those using Box-Plots. The method used to calculate the cut-off value of the spatial navigation performance based on VISSPAT sum score was detailed in the manuscript. (1)

In order to compare the VISSPAT sum score-based data published in the manuscript (1) with non-published study partner-reported data of the same included population, I calculated and visualized using bar graphs the repartition of “continuous” SP-VISSPAT sum score, “continuous” SP-VISSAT (3-8) sum score, and “continuous” VISSPAT (3-8), as previously described. Moreover, I additionally reported and visualized here the repartition of self-reported MEMORY-, and LANGUAGE sum scores.

At a first step, I evaluated each of the additional sum score as fixed variable using linear regression. The predictor variables were the same as in the manuscript and will be detailed at each stage of the analysis. (1) For the same reason as in the manuscript, (1) sex was not included as covariable in this work,

neither, even though it is considered a demographic skill which might interfere with the spatial orientation. (56)

For the comparability of the data, regression analysis followed, here too, two strategies. First, all predictors were inserted in the evaluation, then a stepwise withdrawal (entry p=0.050, removal p=0.075) was evaluated. (1)

At a further step, I performed a multivariate (MANOVA) and univariate (ANOVA) analyses of variance, based on the “continuous” VISSPAT sum score (in contrary to the manuscript, where “dichotomized” VISSPAT sum score based on the cutoff value was applied). (1) Details about variables will be presented at each stages. Additionally, I performed the same analyses based on the “continuous” SP-VISSPAT sum score in relation to BA 34 GMV and FDGu.

Adjusted R2 was already defined in the manuscript, and is “the proportion of the variance of the dependent variable that was explained by the model to characterize effect size”. Changes in adjusted R2 characterized the “effect size of the contribution of individual predictor variables”. (1)

Differently from the manuscript, where the statistical analyses were performed using SPSS, (1) here I used STATA 15 for all statistical analyses and generation of graphics.

5. Results

5.1. Included cases

The strategy used to include cases was already reported in the published manuscript, and is reported here, too, for a clearer overview. (1) Among the 458 patients, 17.20% met one or more exclusion criteria. None of the patients presented with a FDG-PET imaging missing the complete coverage of the pons. VISSPAT subscores were incompletely collected in 7.00% of cases, while a considerable delay of more than 30 days between the date of PET scan and neuropsychological testing of ECog was found in 7.20% of cases. (1)

Based on the definition of outliers previously detailed, 3.10% and 3.30% of cases were considered outliers based on their neuroimaging findings in BA 28 and BA 34, respectively. (1)

Following this strategy, 379 ADNI participants were eligible for our study. (Figure 3).

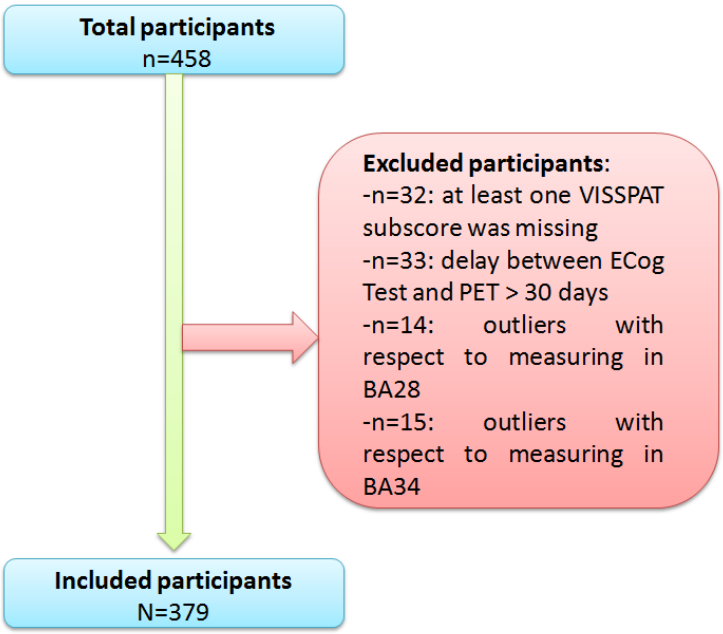

Figure 3: Flow chart of the study

5.2. Age at PET

The mean age of participants included in this study was 71.50±7.40 years, (1) and it ranged between 55 and 91 years (figure 4). Only one patient aged over 90 (0.26%), 49 aged between 80 and 89 (12.93%), 169 aged between 70 and 79 (44.59%), 138 aged between 60 and 69 (36.41%), and 22 were strictly under the age of 60 (5.80%).

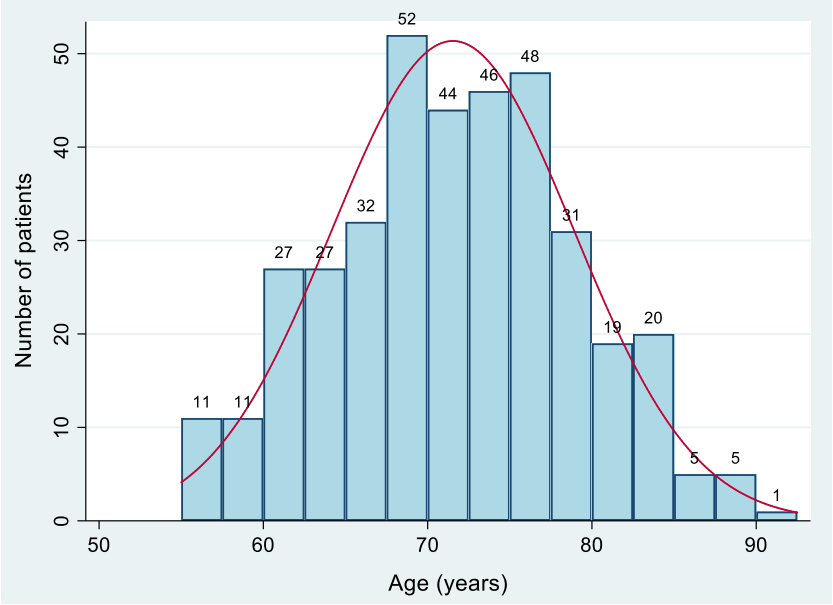

Figure 4: Age repartition in included MCI study patients.

5.3. Sex

Females represented 43% of our population, while 57% were males (figure 5). (1)

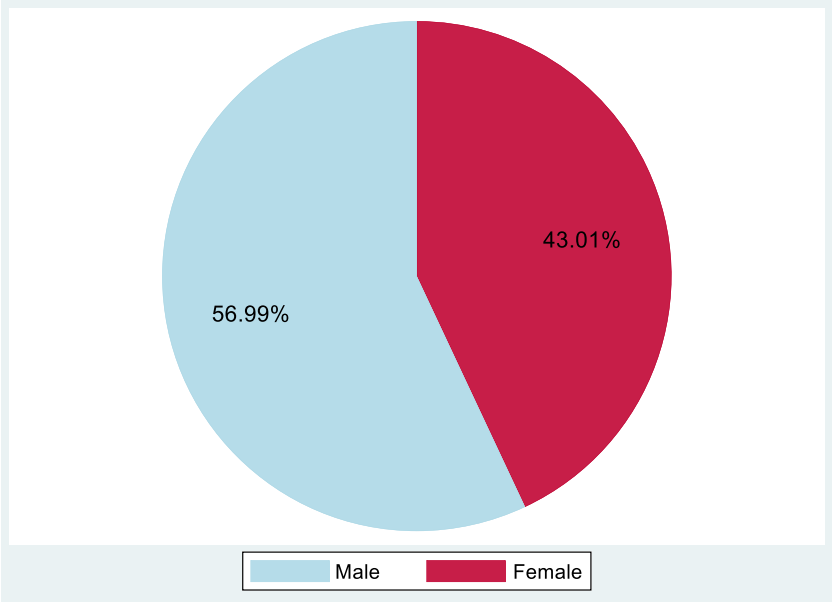

Figure 5: Sex repartition in MCI study patients.

The mean age was 70.40±7.87 in the female group; and 72.38±6.84 in the male group (figure 6). There was a significant difference in between groups, with males being significantly older than females (p=0.009).

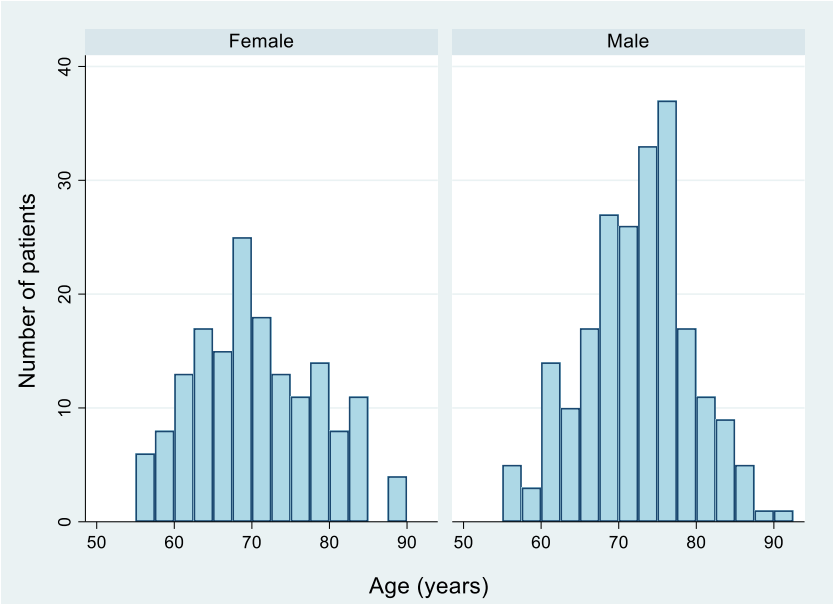

Figure 6: Age repartition according to sex groups.

5.4. APOE4 profile

In 48.30% of cases, the APOE4 profile was positive; while 51.06% had a negative APOE4 profile. (1) The repartition based on the number of APOE4 alleles is shown in figure 7.

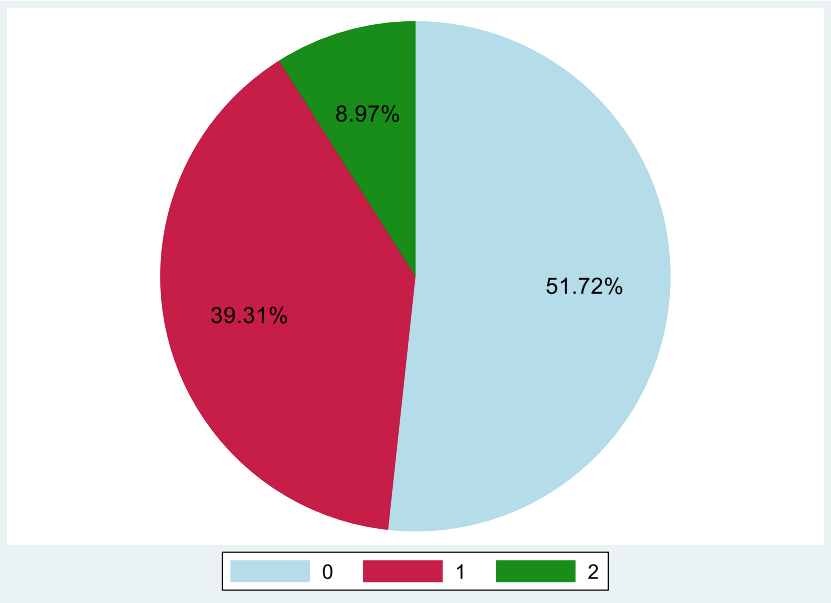

Figure 7: Repartition of APOE4 alleles in MCI study patients.

5.5. Educational level

Included patients had an average of 16.30±2.60 years of education. (1) The educational level ranged between 10 and 20 years (figure 8).

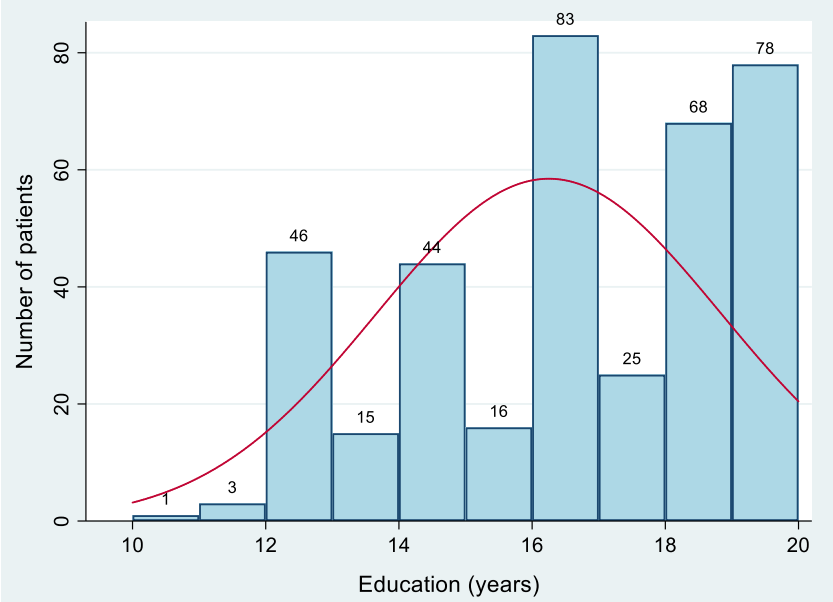

Figure 8: Repartition of educational level (years) in MCI study patients.

5.6. ADAS13 score at baseline

The average ADAS13 score of included cases was 14.80±6.70, and ranged between two and thirty-eight (figure 9). (1)

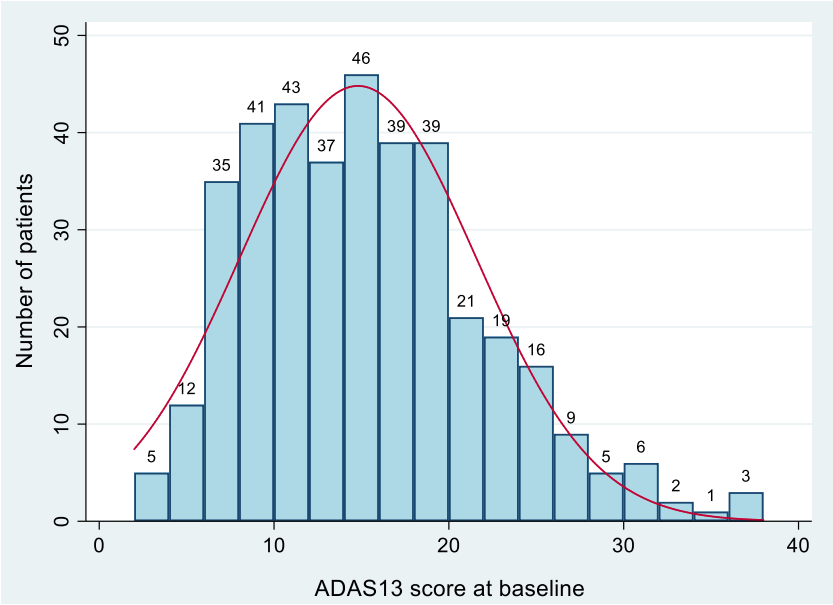

Figure 9: Repartition of ADAS13 scores at baseline in MCI study patients.

5.7. Visuospatial domain of ECog (VISSPAT): Self-reported

5.7.1. VISSPAT 1: "Following a map to find a new location"

VISSPAT1 score was equal to one in 63.59%, two in 23.75%, three in 9.50% and four in 3.17% of cases (figure 10). There was no significant difference neither in BA 34 GMV (p=0.06) or BA 28 GMV (p=0.08), nor in BA 34 FDGu (p=0.57) or BA 28 FDGu (p=0.65) between patients with preserved spatial orientation (VISSPAT 1 = 1) on one side, and impaired spatial orientation (VISSPAT 1 > 1) on the other side based on VISSPAT 1 score (figure 11).

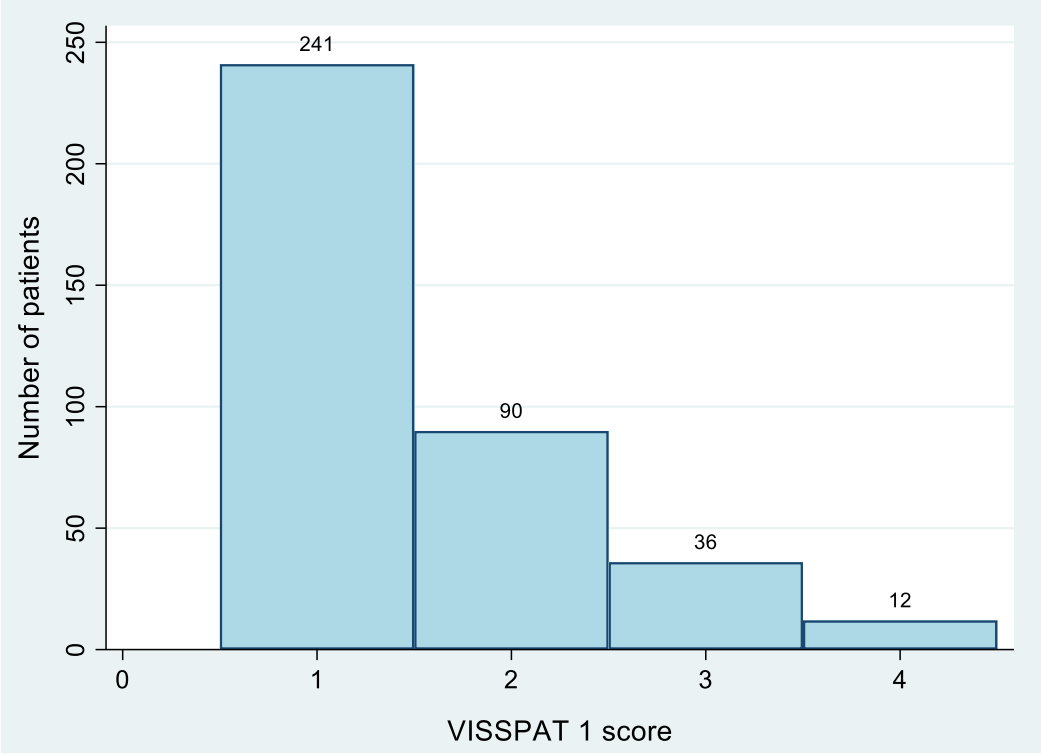

Figure 10: Repartition of VISSPAT 1 scores between MCI study patients.

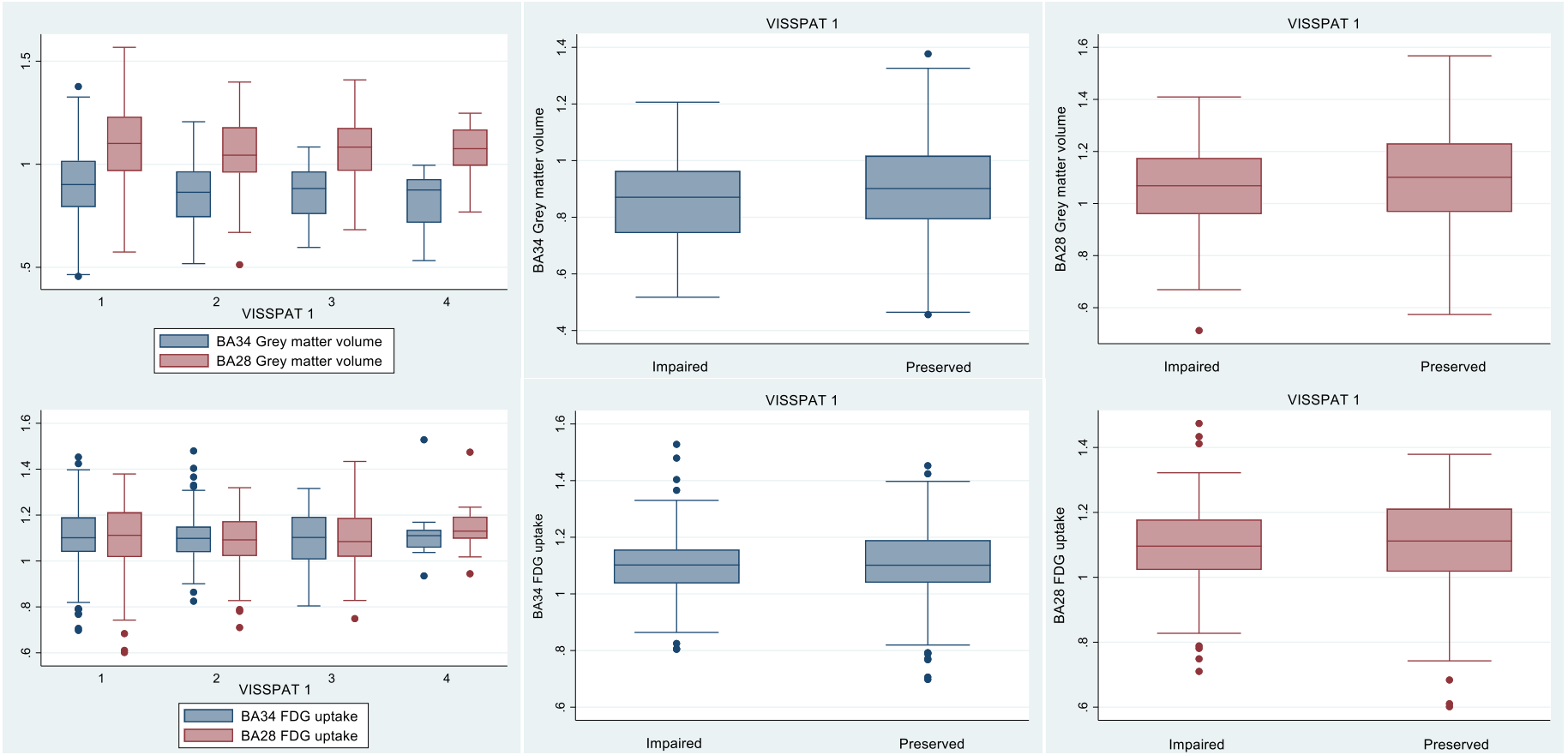

Figure 11: Box plots of repartition of BA 34 FDG uptake and grey matter volume (blue) and BA 28 FDG uptake and grey matter volume (red) based on different VISSPAT 1 subscores (1, 2, 3, and 4) and VISSPAT 1 subgroups (impaired vs. preserved).

5.7.2. VISSPAT 2: "Reading a map and helping with directions when someone else is driving"

VISSPAT 2 score was equal to one in 69.66%, two in 17.15%, three in 8.44% and four in 4.75% of cases (figure 12). There was no significant difference neither in BA 34 GMV (p=0.13) or BA 28 GMV (p=0.37) nor in BA 34 FDGu (p=0.23) or BA 28 FDGu (p=0.20) between patients with preserved spatial orientation (VISSPAT 2 = 1) on one side and impaired spatial orientation (VISSPAT 2 > 1) on the other side based on VISSPAT 2 score (figure13).

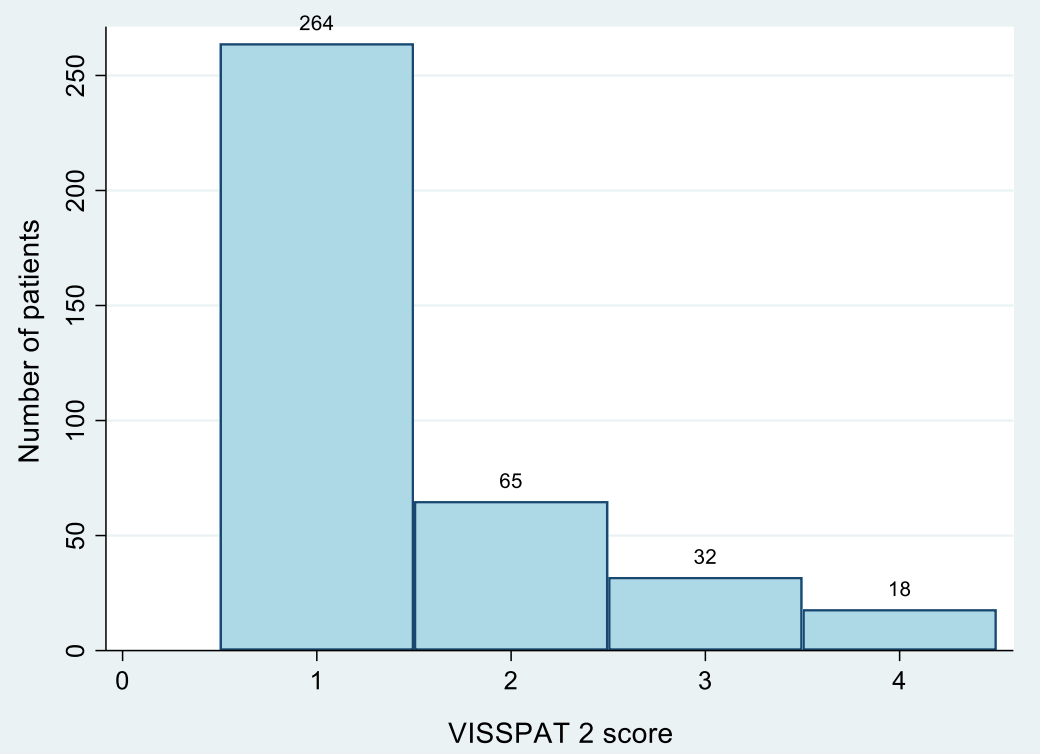

Figure 12: Repartition of VISSPAT 2 scores between MCI study patients.

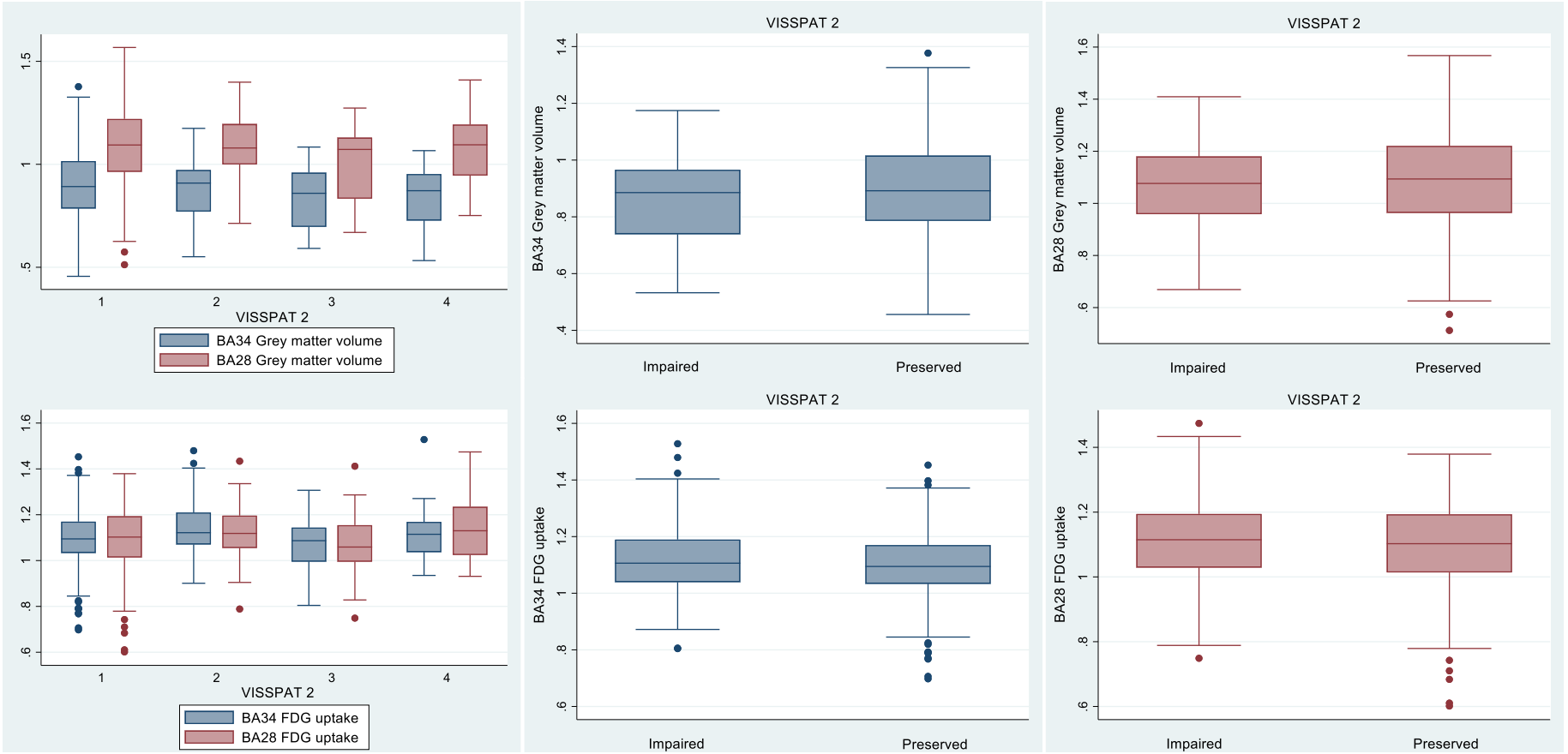

Figure 13: Box plots of repartition of BA 34 FDG uptake and grey matter volume (blue) and BA 28 FDG uptake and grey matter volume (red) based on different VISSPAT 2 subscores (1, 2, 3, and 4) and VISSPAT 2 subgroups (impaired vs. preserved).

5.7.3. VISSPAT 3: “Finding my car in a parking lot”

VISSPAT 3 score was equal to one in 48.28%, two in 35.36%, three in 13.46% and four in 2.90% of cases (figure 14). There was no significant difference neither in BA 34 GMV (p=0.90) or BA 28 GMV (p=0.81) nor in BA 34 FDGu (p=0.53) or BA 28 FDGu (p=0.29) between patients with preserved spatial orientation (VISSPAT 3 = 1) on one side and impaired spatial orientation (VISSPAT 3 > 1) on the other side based on VISSPAT 3 score (figure 15).

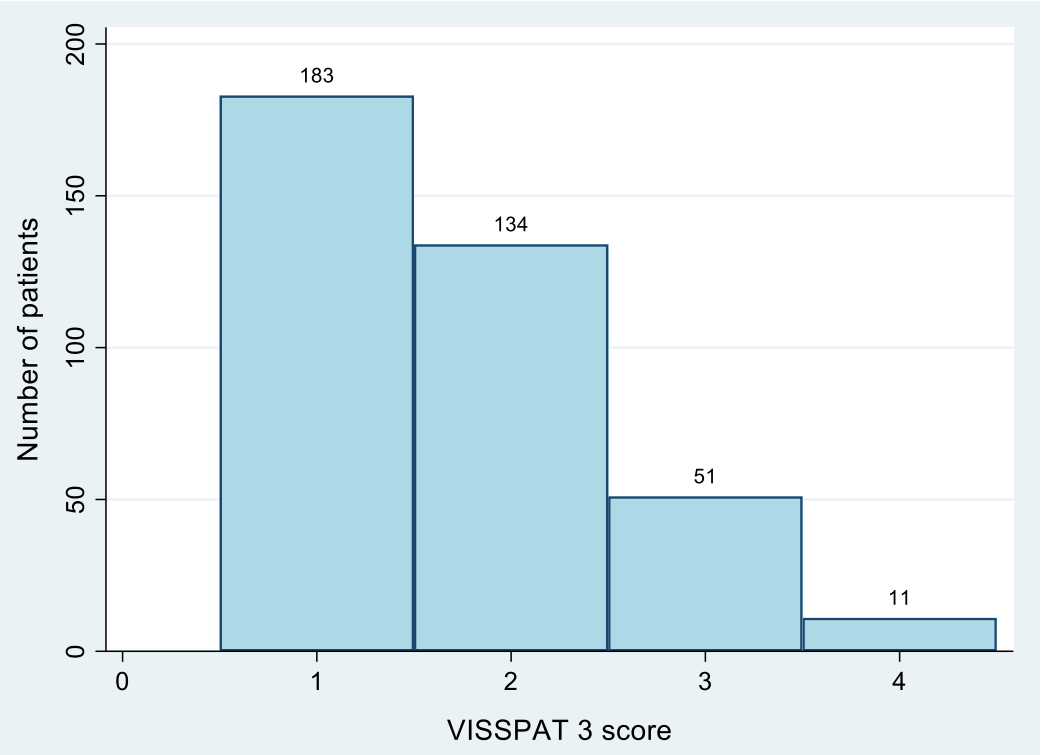

Figure 14: Repartition of VISSPAT 3 scores between MCI study patients.

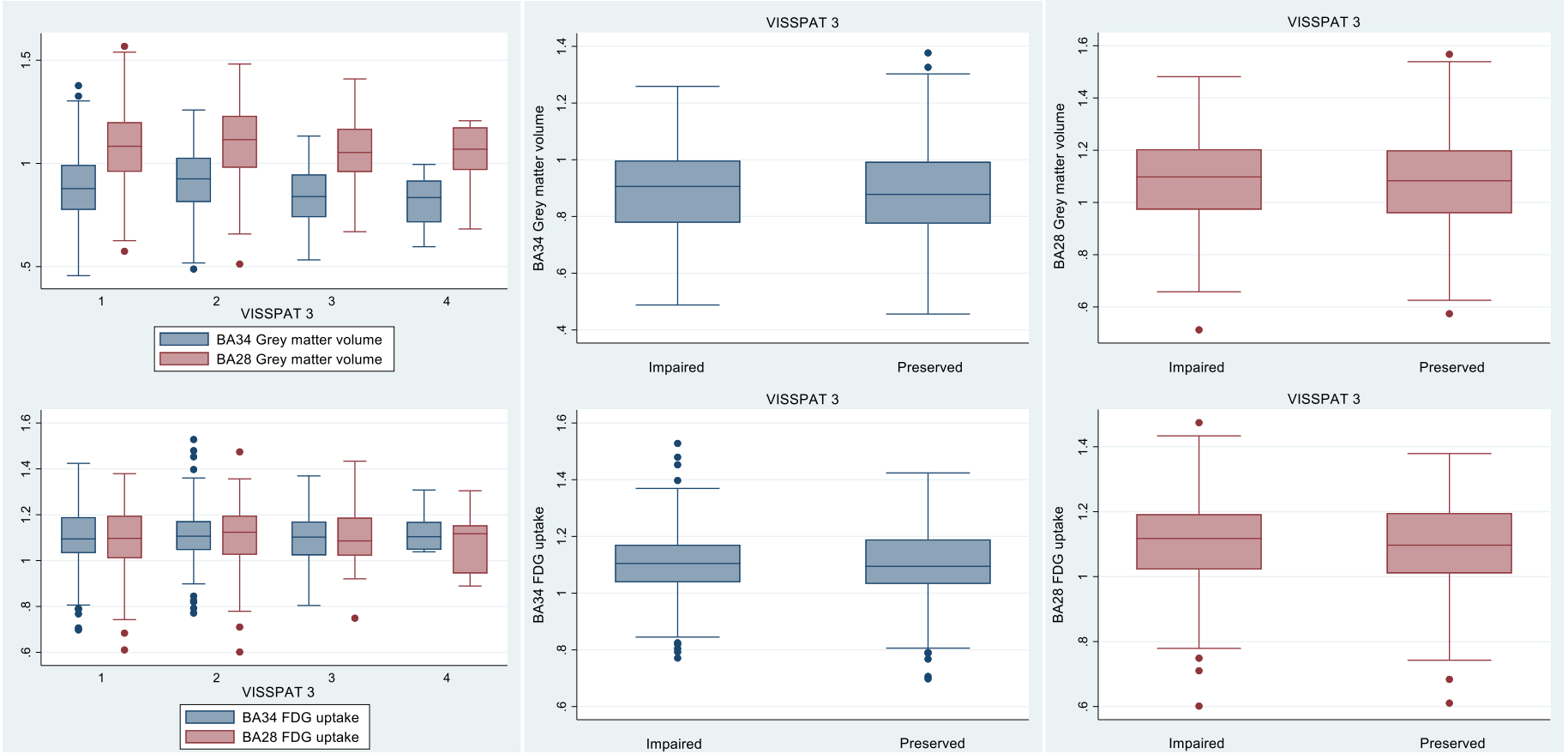

Figure 15: Box plots of repartition of BA 34 FDG uptake and grey matter volume (blue) and BA 28 FDG uptake and grey matter volume (red) based on different VISSPAT 3 subscores (1, 2, 3, and 4) and VISSPAT 3 subgroups (impaired vs. preserved).

5.7.4. VISSPAT 4: "Finding my way back to a meeting spot in the mall or other location"

VISSPAT4 score was equal to one in 58.05%, two in 27.44%, three in 11.87% and four in 2.64% of cases (figure 16). There was no significant difference neither in BA 34 GMV (p= 0.15) or BA 28 GMV (p= 0.10) nor in BA 34 FDGu (p=0.11) or BA 28 FDGu (p= 0.33) between patients with preserved spatial orientation (VISSPAT 4 = 1) on one side and patients with impaired spatial orientation (VISSPAT 4 > 1) on the other side based on VISSPAT 4 score (figure 17).

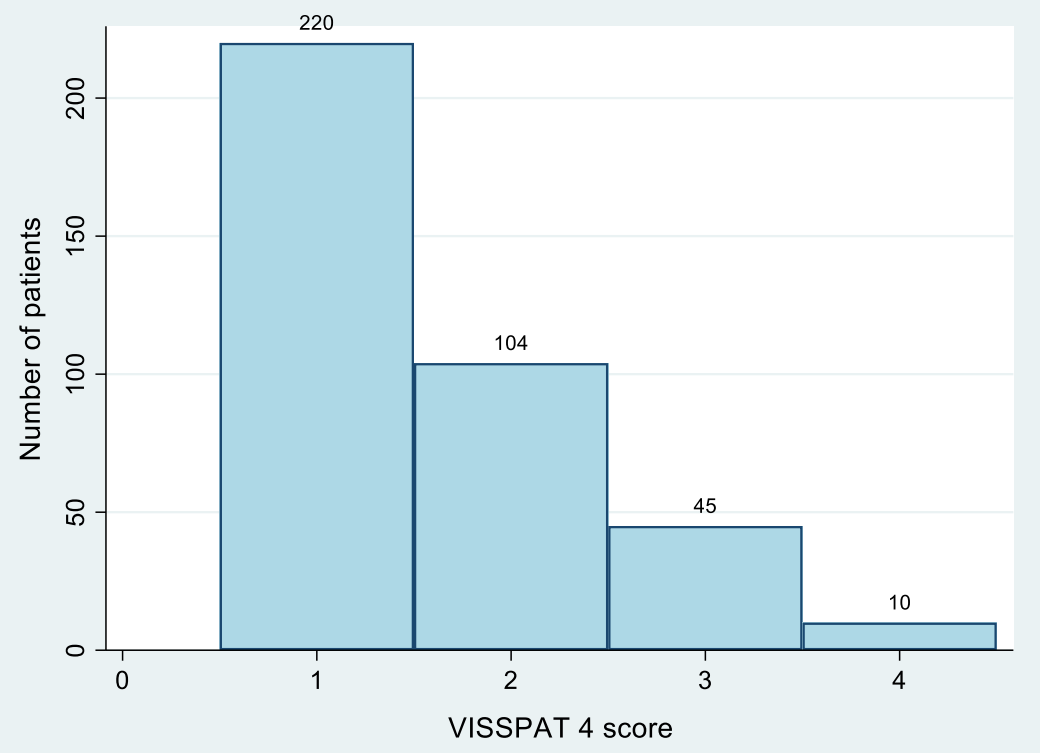

Figure 16: Repartition of VISSPAT 4 scores between MCI study patients.

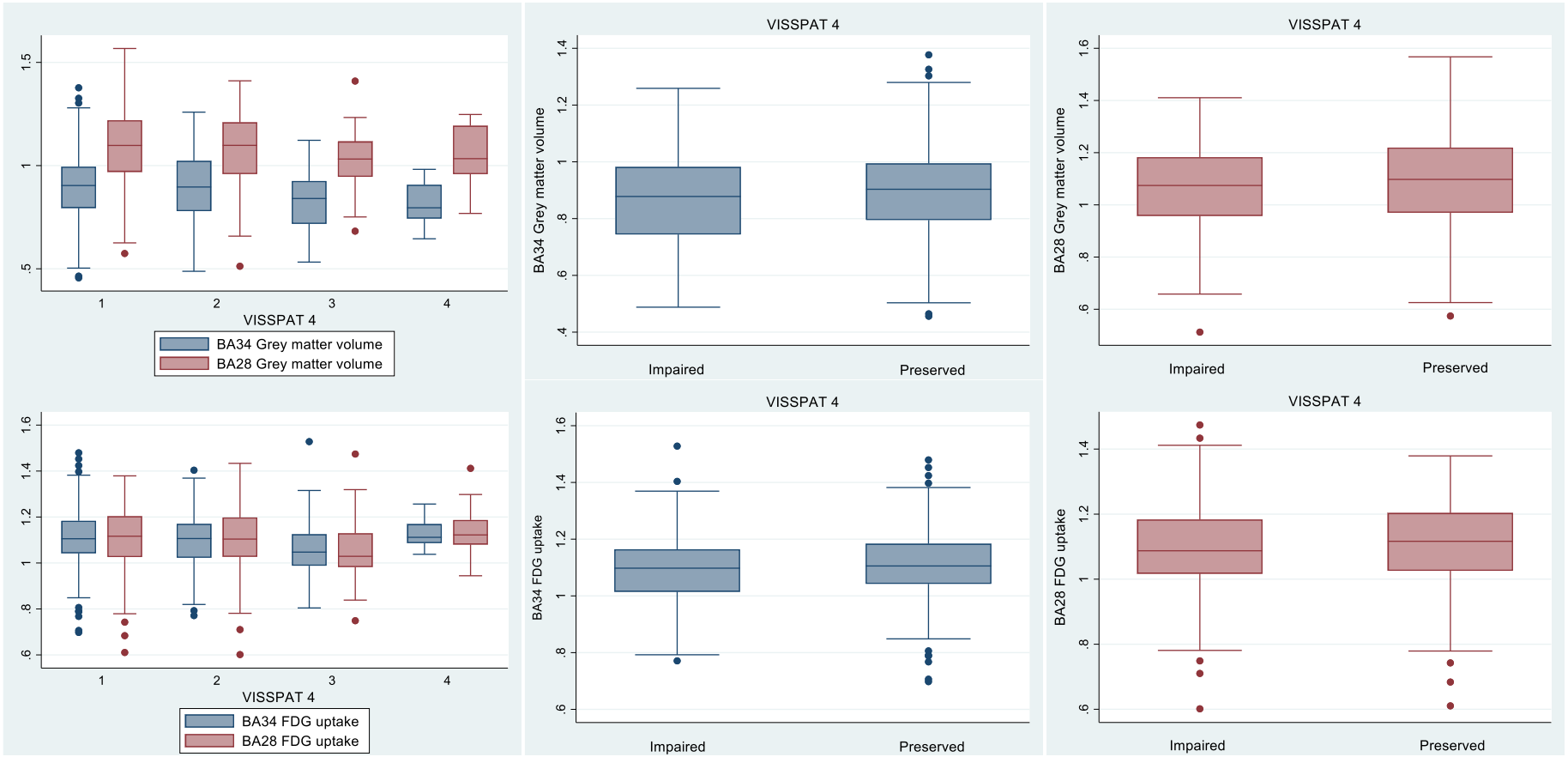

Figure 17: Box plots of repartition of BA 34 FDG uptake and grey matter volume (blue) and BA 28 FDG uptake and grey matter volume (red) based on different VISSPAT 4 subscores (1, 2, 3, and 4) and VISSPAT 4 subgroups (impaired vs. preserved).

5.7.5. VISSPAT 6: "Finding my way around a familiar neighborhood"

VISSPAT 6 score was equal to one in 79.16%, two in 15.30%, three in 5.01% and four in 0.53% of cases (figure 18). The BA 34 GMV was significantly higher in patients with preserved spatial orientation than in those with impaired spatial orientation (p=0.03, mean=0.89±0.17 vs. 0.85±0.14, respectively) in this sub-domain. There was no significant difference neither in BA 28 GMV (p= 0.20) nor in BA 34 FDGu (p= 0.55) or BA 28 FDGu (p=0.40) between patients with preserved spatial orientation (VISSPAT 6 = 1) on one side and impaired spatial orientation (VISSPAT 6 > 1) on the other side based on VISSPAT 6 score (figure 19).

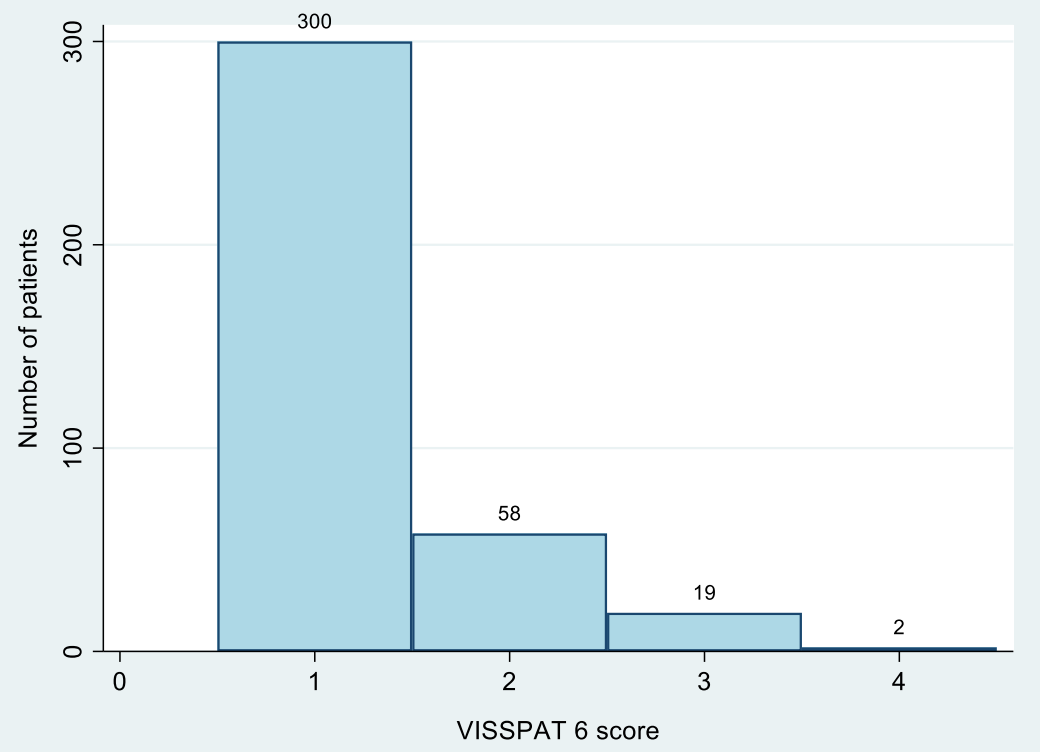

Figure 18: Repartition of VISSPAT 6 scores between MCI study patients.

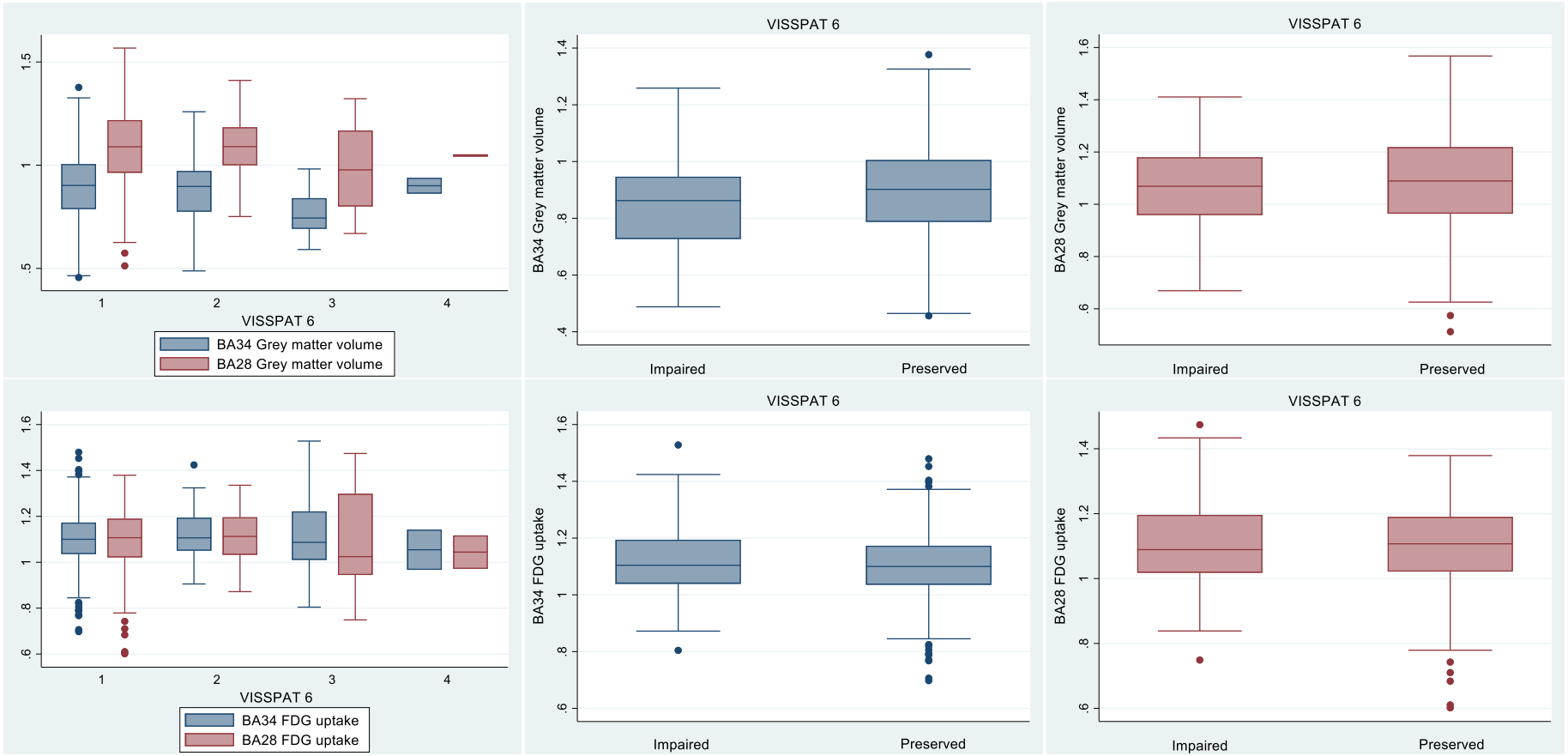

Figure 19: Box plots of repartition of BA 34 FDG uptake and grey matter volume (blue) and BA 28 FDG uptake and grey matter volume (red) based on different VISSPAT 6 subscores (1, 2, 3, and 4) and VISSPAT 6 subgroups (impaired vs. preserved).

5.7.6. VISSPAT 7: “Finding my way around a familiar store”

VISSPAT 7 score was equal to one in 76.78%, two in 16.89%, three in 5.80% and four in 0.53% of cases (figure 20). The BA 34 GMV was significantly higher in patients with preserved spatial orientation than those with impaired spatial orientation (p=0.05, mean=0.89±0.17 vs. 0.86±0.14, respectively) in this sub-domain. There was no significant difference neither in BA 28 GMV (p=0.30) nor in BA 34 FDGu (p=0.87) or BA 28 FDGu (p=0.77) between patients with preserved spatial orientation (VISSPAT 7 = 1) on one side and impaired spatial orientation (VISSPAT 7 > 1) on the other side based on VISSPAT 7 score (figure 21).

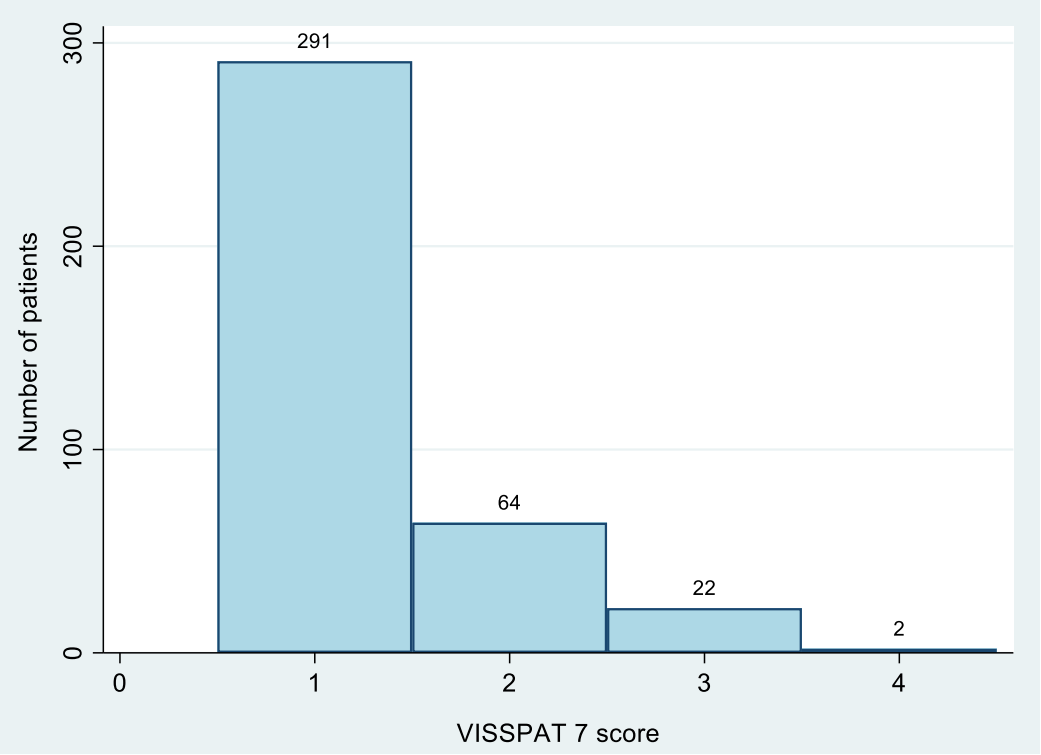

Figure 20: Repartition of VISSPAT 7 scores between MCI study patients.

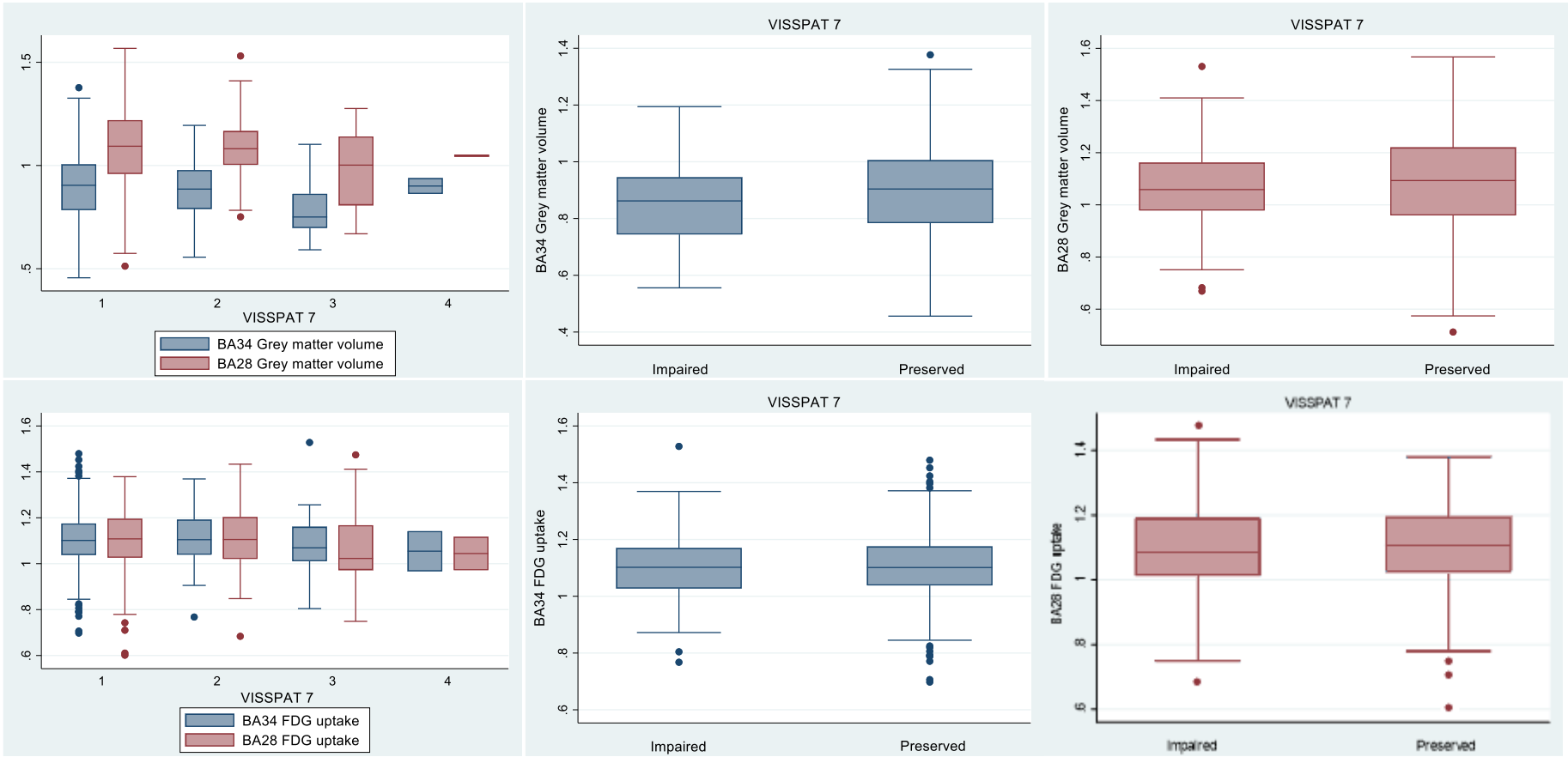

Figure 21: Box plots of repartition of BA 34 FDG uptake or grey matter volume (blue) and BA 28 FDG uptake and grey matter volume (red) based on different VISSPAT 7 subscores (1, 2, 3, and 4) and VISSPAT 7 subgroups (impaired vs. preserved).

5.7.7. VISSPAT 8: “Finding my way around a house visited many times”

VISSPAT 8 score was equal to one in 86.02%, two in 10.55%, three in 3.17% and four in 0.26% of cases (figure 22). The BA 34 GMV was significantly higher in patients with preserved spatial orientation than those with impaired spatial orientation (p=0.01, mean=0.89±0.16 vs. 0.84±0.16, respectively) in this sub-domain. The same observation was retained regarding BA 28 (p=0.04, mean=1.09±0.18 vs. 1.03±0.2). There was no significant difference in BA 34 FDGu (p=0.74) or BA 28 FDGu (p=0.34) between patients with preserved spatial orientation (VISSPAT 8 = 1) on one side and impaired spatial orientation (VISSPAT 8 > 1) on the other side based on VISSPAT 8 score (figure 23).

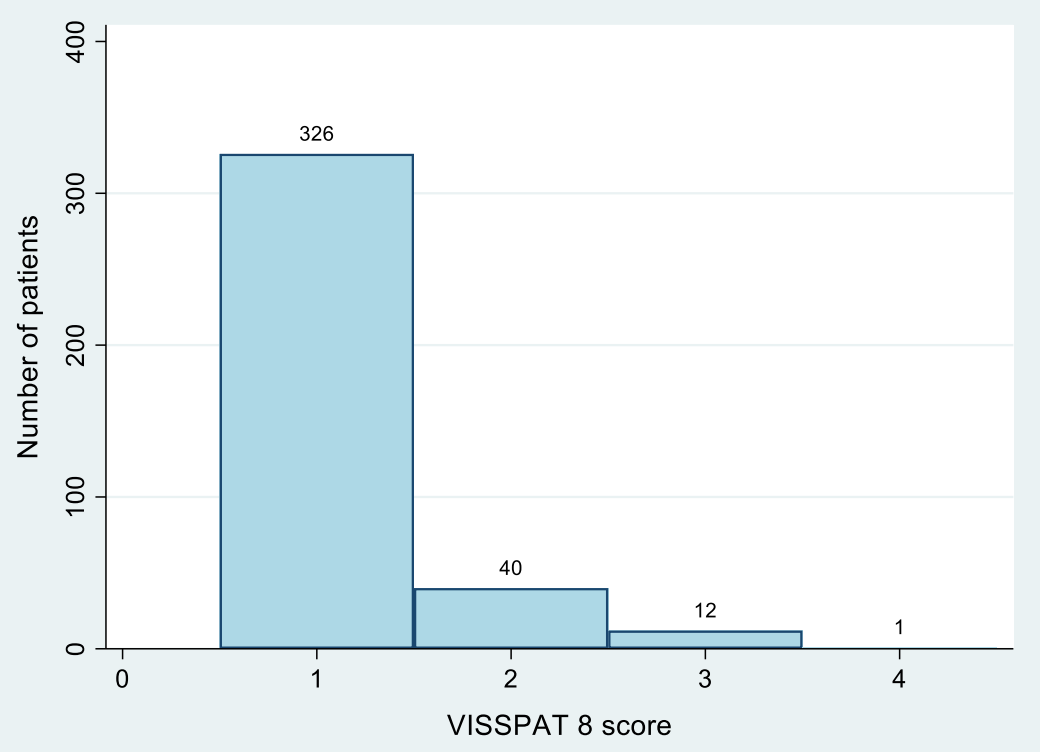

Figure 22: Repartition of VISSPAT 8 scores between MCI study patients.

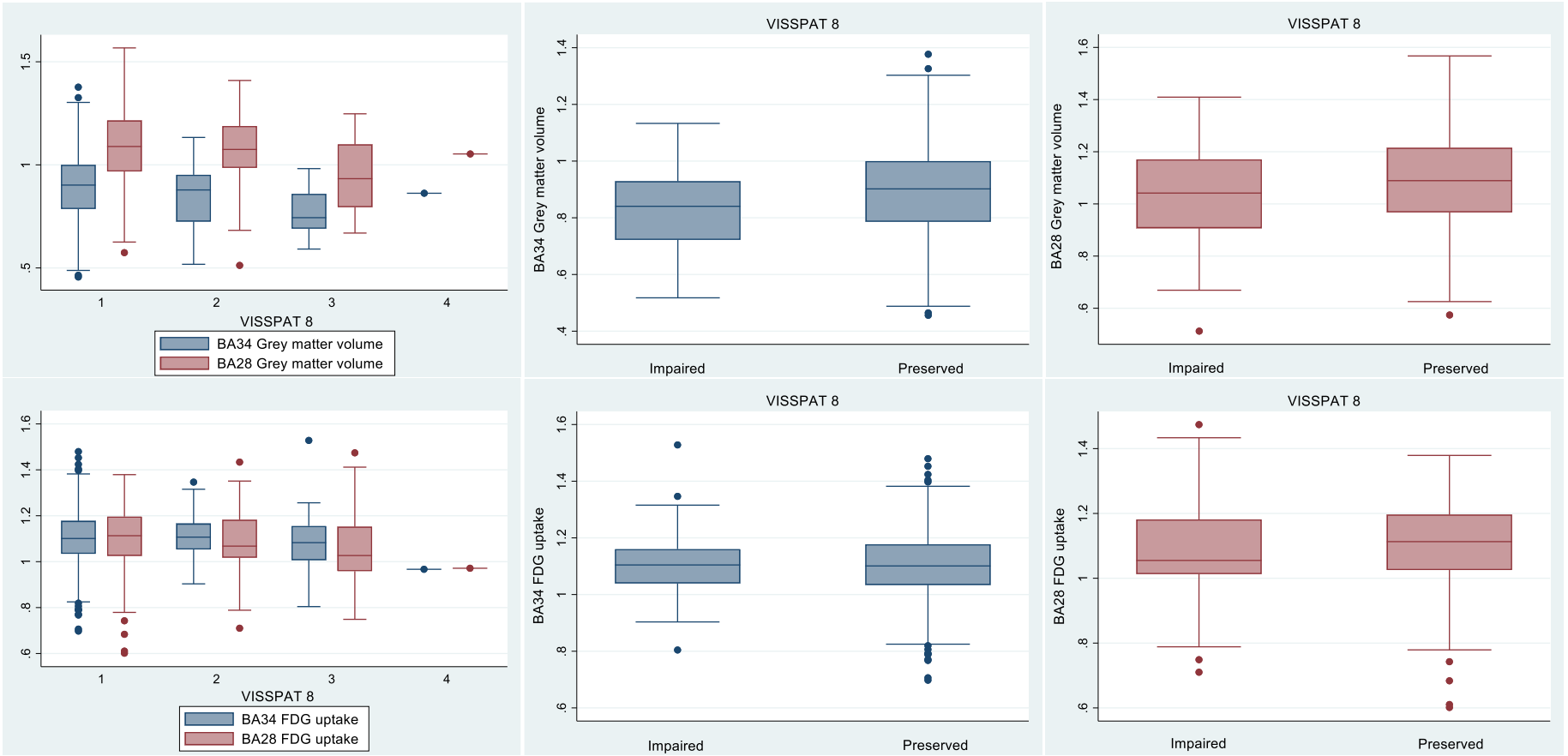

Figure 23: Box plots of repartition of BA 34 FDG uptake and grey matter volume (blue) and BA 28 FDG uptake and grey matter volume (red) based on different VISSPAT 8 subscores (1, 2, 3, and 4) and VISSPAT 8 subgroups (impaired vs. preserved).

5.8. BA 34 Grey matter volume

The mean BA 34 GMV in patients with preserved spatial orientation based on the VISSPAT sum score's cut-off value was 0.90±0.17 and ranged from 0.46 to 1.38, while in patients with altered spatial orientation, based on the same reference value, it was lower with a mean of 0.87±0.15 and ranged from 0.49 to 1.26 (figure 24). The difference between the two groups was statistically not significant (p=0.07).

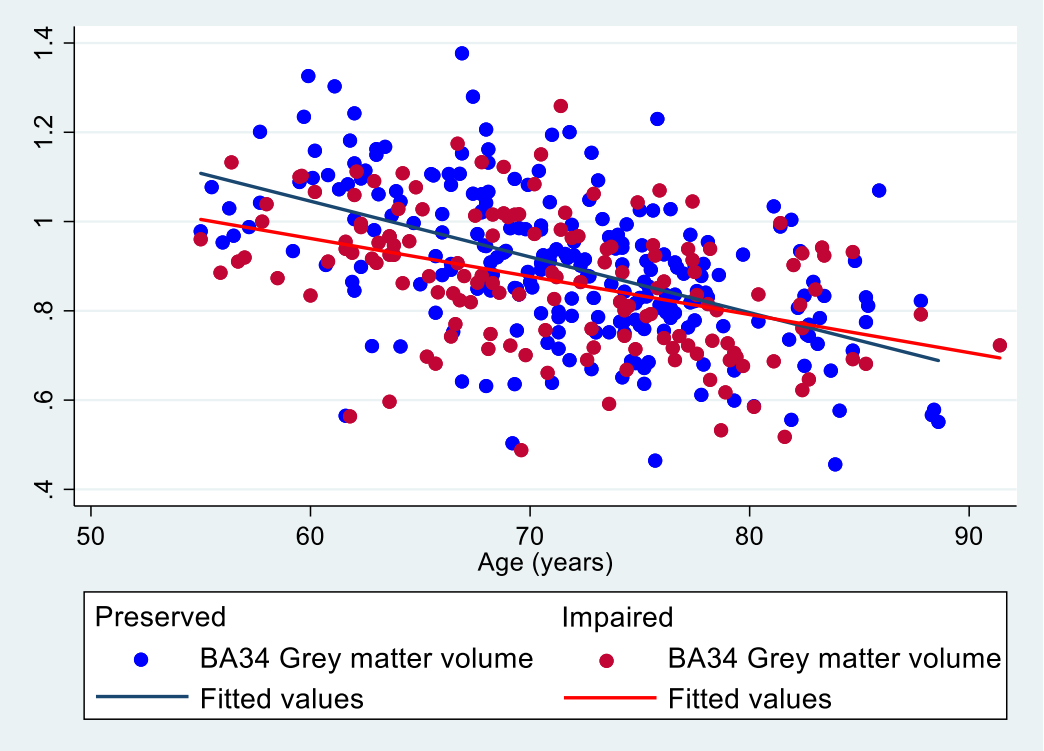

Figure 24: Repartition of BA 34 Grey matter volume based on age (years) in MCI study patients with preserved and impaired spatial orientation.

5.9. BA 34 FDG uptake

The mean BA 34 FDGu in patients with preserved spatial orientation based on the VISSPAT sum score's cut-off value was 1.10±0.13 and ranged from 0.70 to 1.45, while in patients with altered spatial orientation, based on the same reference value, it was almost identical with a mean of 1.11±0.13 and ranged from 0.80 to 1.53 (figure 25). The difference between the two groups was statistically not significant (p=0.67).

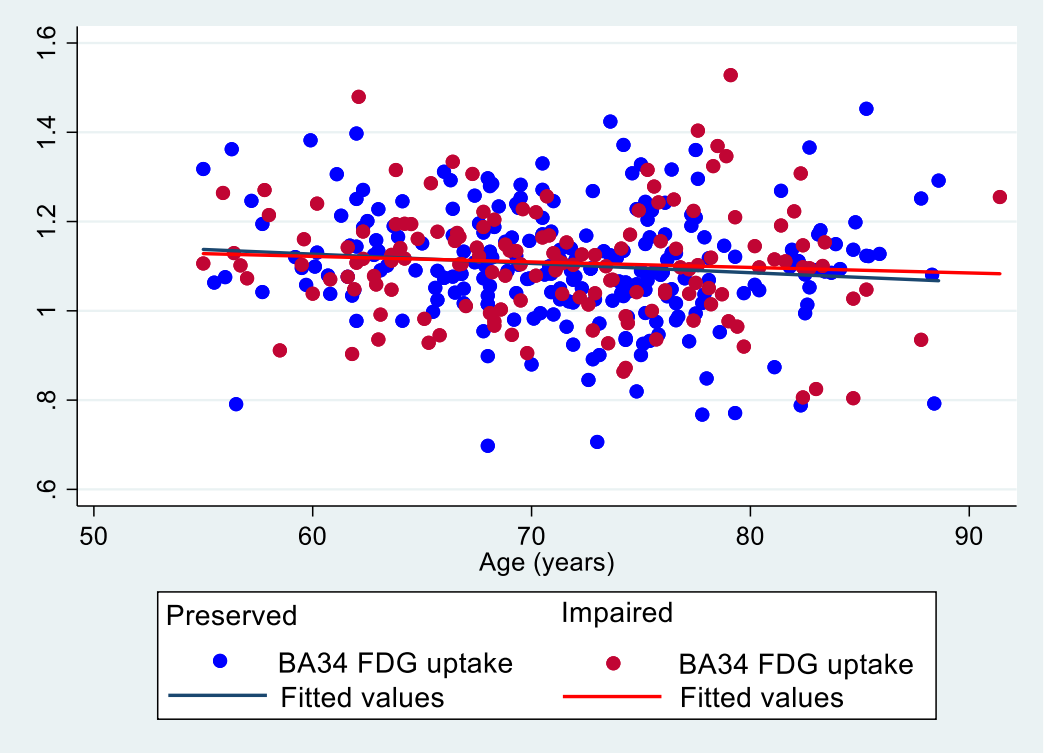

Figure 25: Repartition of BA 34 FDG uptake based on age (years) in MCI study patients with preserved and impaired spatial orientation.

5.10. BA 28 Grey matter volume

The mean BA 28 GMV in patients with preserved spatial orientation based on the VISSPAT sum score's cut-off value was 1.09±0.20 and ranged from 0.57 to 1.57, while in patients with altered spatial orientation, based on the same reference value, it was lower with a mean of 1.06±0.17 and ranged from 0.51 to 1.41 (figure 26). The difference between the two groups was statistically not significant (p=0.15).

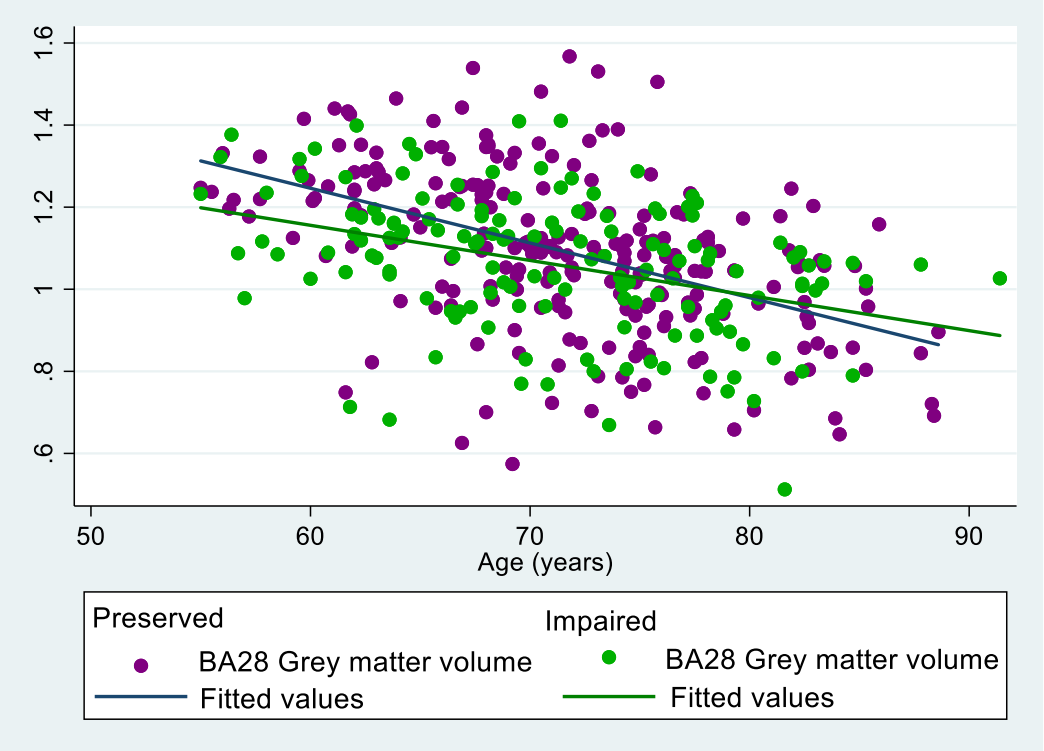

Figure 26: Repartition of BA 28 Grey matter volume based on age (years) in MCI study patients with preserved and impaired spatial orientation.

5.11. BA 28 FDG uptake

The mean BA 28 FDGu in patients with preserved spatial orientation based on the VISSPAT sum score's cut-off value was 1.10±0.14 and ranged from 0.60 to 1.38, while in patients with altered spatial orientation, based on the same reference value, it was identical with a mean of 1.10±0.13 and ranged from 0.71 to 1.47 (figure 27). The difference between the two groups was statistically not significant (p=0.588).

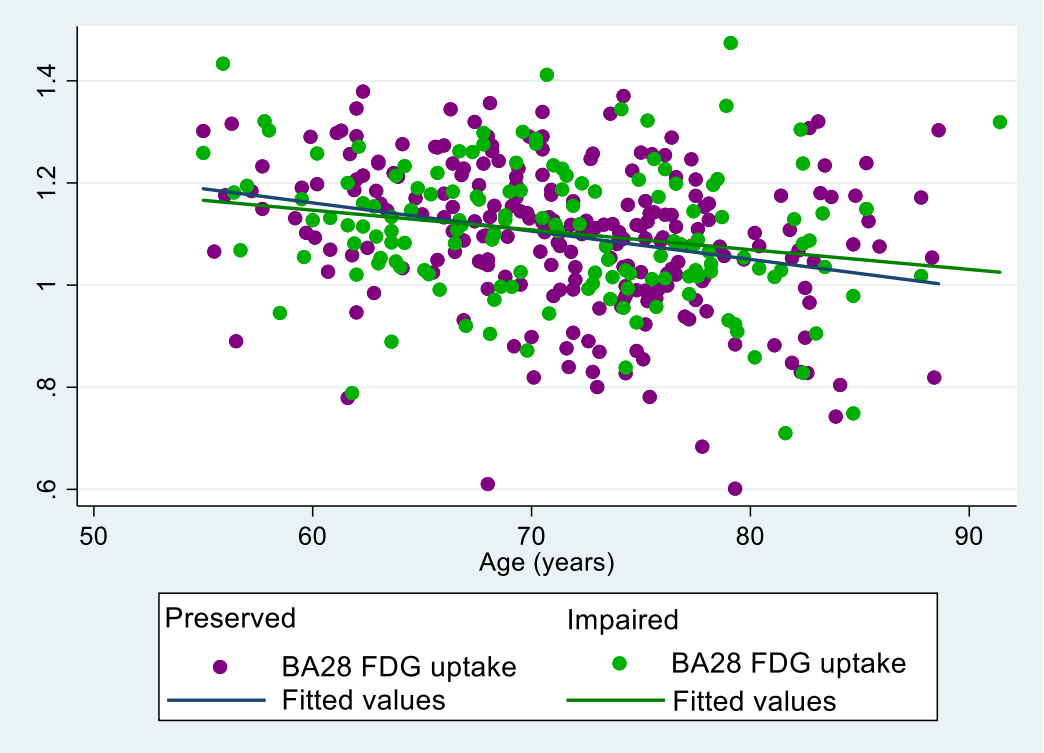

Figure 27: Repartition of BA 28 FDG uptake based on age (years) in MCI study patients with preserved and impaired spatial orientation.

5.12. SP-VISSPAT sum score

Adding all SP-VISSPAT subscores per patient then subtracting seven allowed obtaining a SP-VISSPAT sum score per patient. Figure 28 represents the distribution of the SP-VISSPAT sum score among included patients. The score ranged from zero to twenty and the median value of the SP-VISSPAT sum score was one.

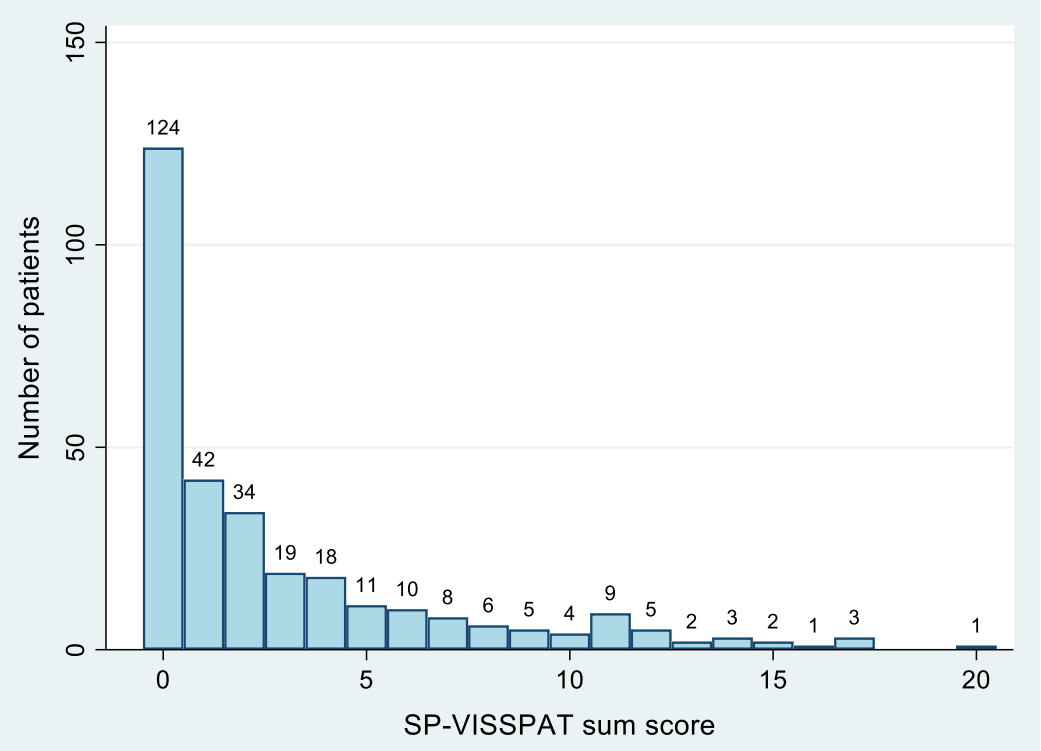

Figure 28: SP-VISSPAT sum score distribution in MCI study patients.

In a further step, and to avoid interference with language and communication abilities of patients toward their partners, SP-VISSPAT (3-8) sum score was calculated by adding SP-VISSPAT subscores three to eight for each patient, then subtracting five. Figure 29 represents the distribution of the SP-VISSPAT (3-8) sum score among included patients. The SP-VISSPAT (3-8) sum score ranged from zero to fourteen and the median value was zero.

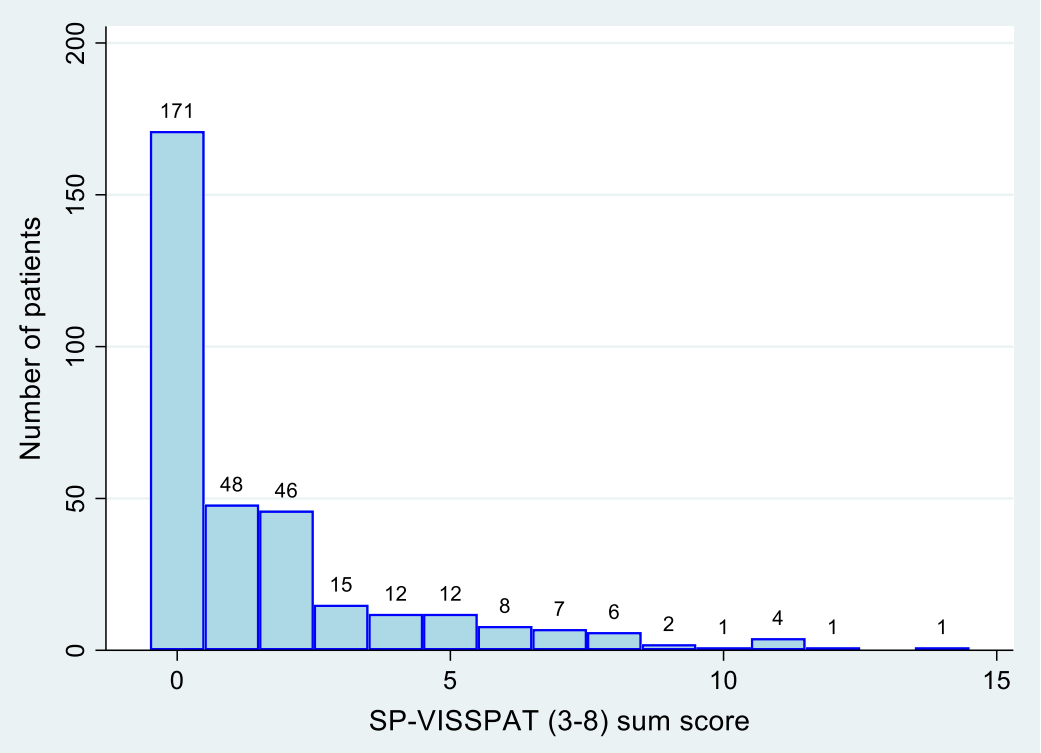

Figure 29: SP-VISSPAT (3-8) sum score distribution in MCI study patients.

In order to compare the study partner-reported with the self-reported results, the same procedure was followed for VISSPAT (3-8) sum score (figure 30).

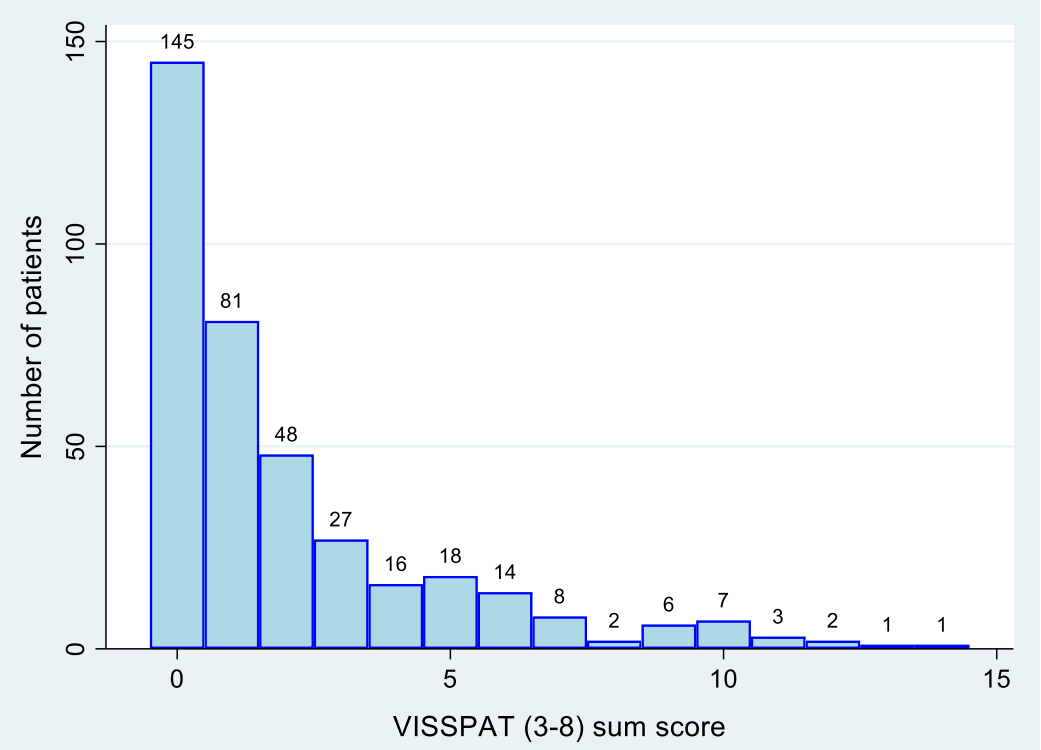

Figure 30: VISSPAT (3-8) sum score distribution in MCI study patients.

5.13. Regression analysis with SP-VISSPAT sum score

The linear regression of the “continuous” SP-VISSPAT sum score in the total sample of MCI patients showed no significant contribution of the predictor variables. The stepwise regression left ADAS13 score (p=0.000). The same observation was obtained with SP-VISSPAT (3-8) sum score. While, similarly to the results published in the manuscript based on the full VISSPAT sum score, (1) VISSPAT (3-8) sum score revealed, here also, a significant model (F=2.51, p=0.011, Adjusted R^2=0.031). The stepwise regression based on VISSPAT (3-8) sum score left BA 34 GMV (p=0.014, β=-0.149), age at PET (p=0.025, β=-0.129) and ADAS13 score (p=0.011, β=0.142) (table1).

Table 1: Regression analysis based on the "continuous" SP-VISSPAT sum score, SP-VISSPAT (3-8) sum score, and VISSPAT (3-8) sum score of included MCI patients. All predictor variables were entered in the model. (*p:* significance, β standardized regression coefficient).

	SP-VISSPAT sum score				**SP-VISSPAT (3-8) sum score**				**VISSPAT (3-8) sum score**			
	Linear regression analysis		Stepwise regression analysis		Linear regression analysis		Stepwise regression analysis		Linear regression analysis		Stepwise regression analysis	
	F=4.21 *p*=0.0001 Adjusted R^2= 0.078		F=30.33 *p*=0.0000 Adjusted R^2=0.088		F=3.63 *p*=0.0005 Adjusted R^2=0.059		F=24.59 *p*=0.000 Adjusted R^2=0.066		F=2.51 *p*=0.011 Adjusted R^2=0.031		F=5.93 *p*=0.000 Adjusted R^2=0.038	
	p	β	*p*	β	*p*	β	*p*	β	*p*	β	*p*	β
BA 28 FDG uptake	0.633	-0.045	■	■	0.700	-0.035	■	■	0.245	0.099	■	■
BA 28 Grey matter volume	0.382	-0.095	■	■	0.238	-0.125	■	■	0.631	0.049	■	■
BA 34 FDG uptake	0.877	0.013	■	■	0.988	-0.001	■	■	0.615	-0.038	■	■
BA 34 Grey matter volume	0.458	0.079	■	■	0.381	0.091	■	■	**0.033**	-0.213	**0.014**	-0.149
Age at PET	0.232	0.076	■	■	0.280	0.067	■	■	**0.034**	-0.126	**0.025**	-0.129
Educational level (years)	0.860	0.010	■	■	0.830	-0.012	■	■	0.814	0.012	■	■
ADAS13 score	0.000	0.251	**0.000**	■	0.001	0.209	**0.000**	■	**0.005**	0.164	**0.011**	0.142
APOE4 profile (binary)	0.474	0.041	■	■	0.471	0.039	■	■	0.790	-0.014	■	■

5.14. MEMORY sum score

Patients who have not answered on all questions of MEMORY domain of ECog were 17 (n=3 for MEMORY 1; n=2 for MEMORY 3; n=9 for MEMORY 5; n=2 for MEMORY 7; and n=1 for MEMORY 8). Only 362 patients had complete MEMORY scores in all subdomains (figure 31). Adding all MEMORY subscores pro patient then subtracting eight allowed obtaining the MEMORY sum score for each patient. The scores ranged from zero to twenty-four, and the median was ten (figure 32).

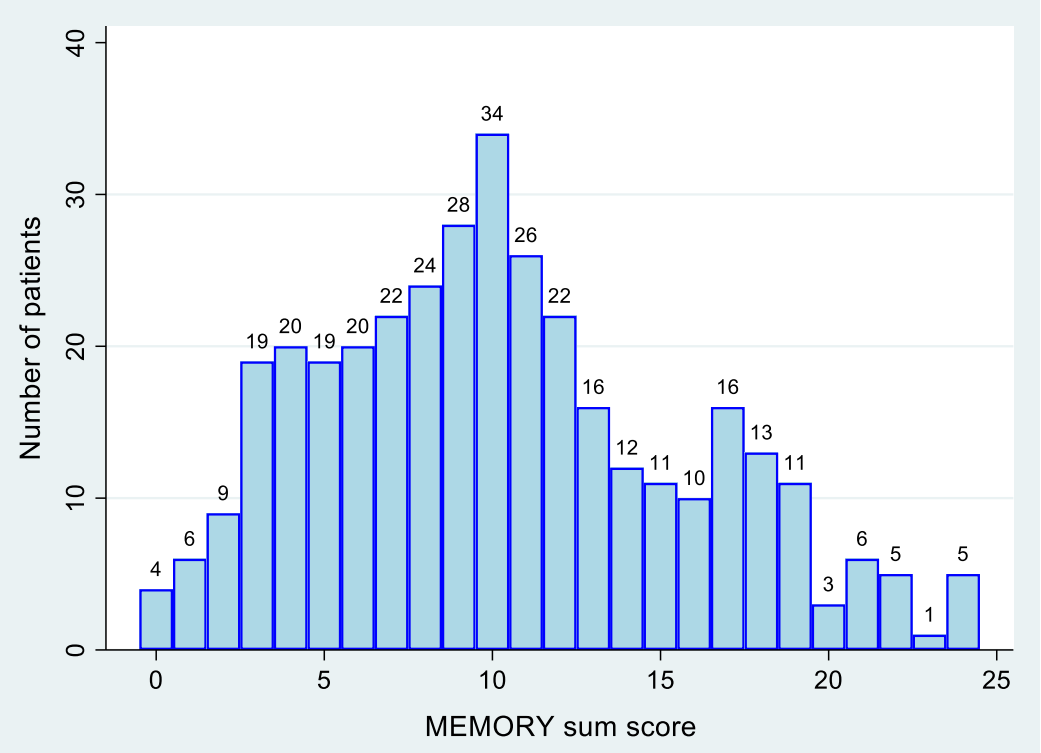

Figure 32: MEMORY sum score distribution in MCI study patients.

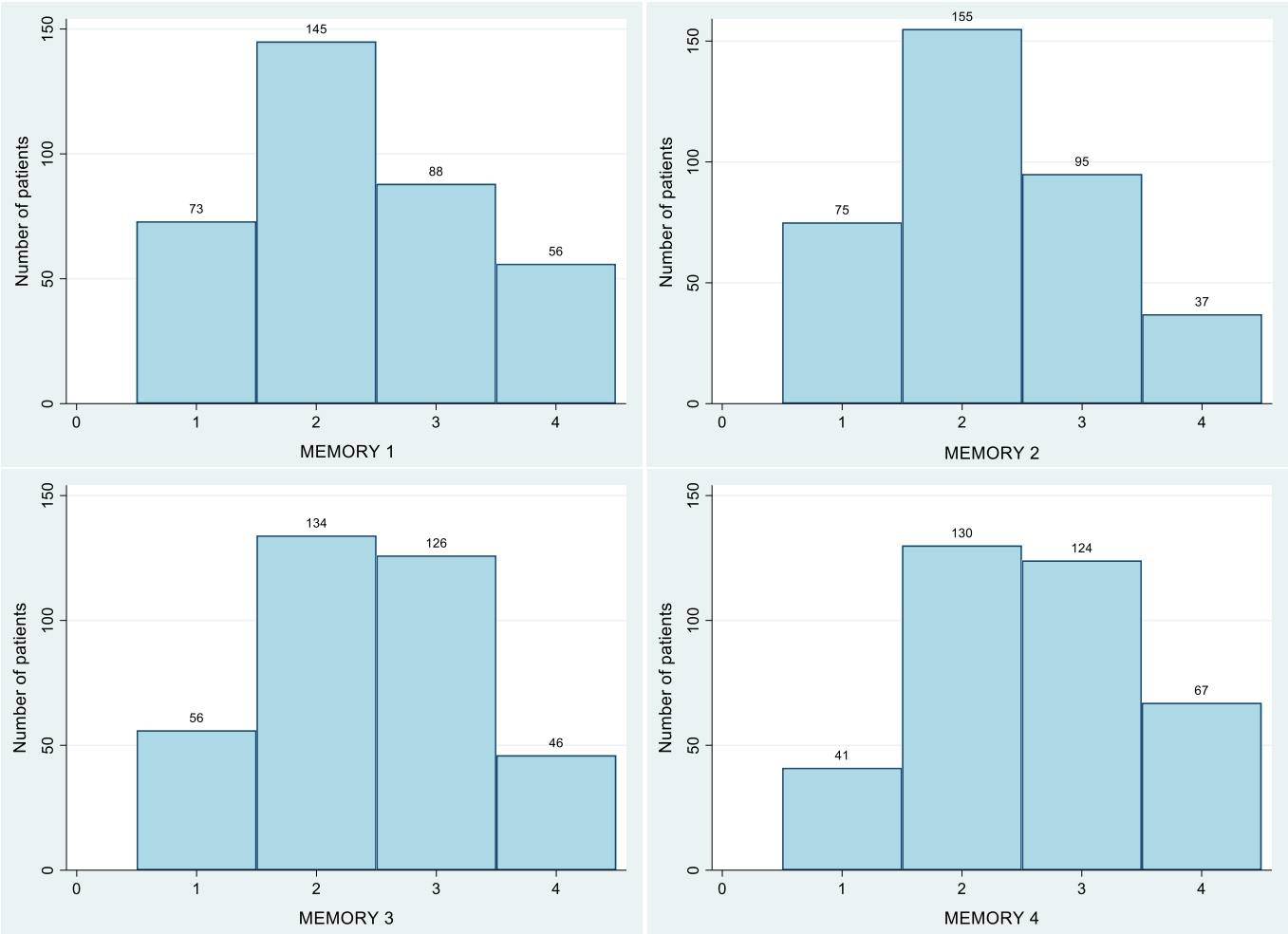
Number of patients
0
50
100
150
0
1
2
3
4
MEMORY 1
73
145
88
56
MEMORY 2
75
155
95
37
MEMORY 3
56
134
126
46
MEMORY 4
41
130
124
67

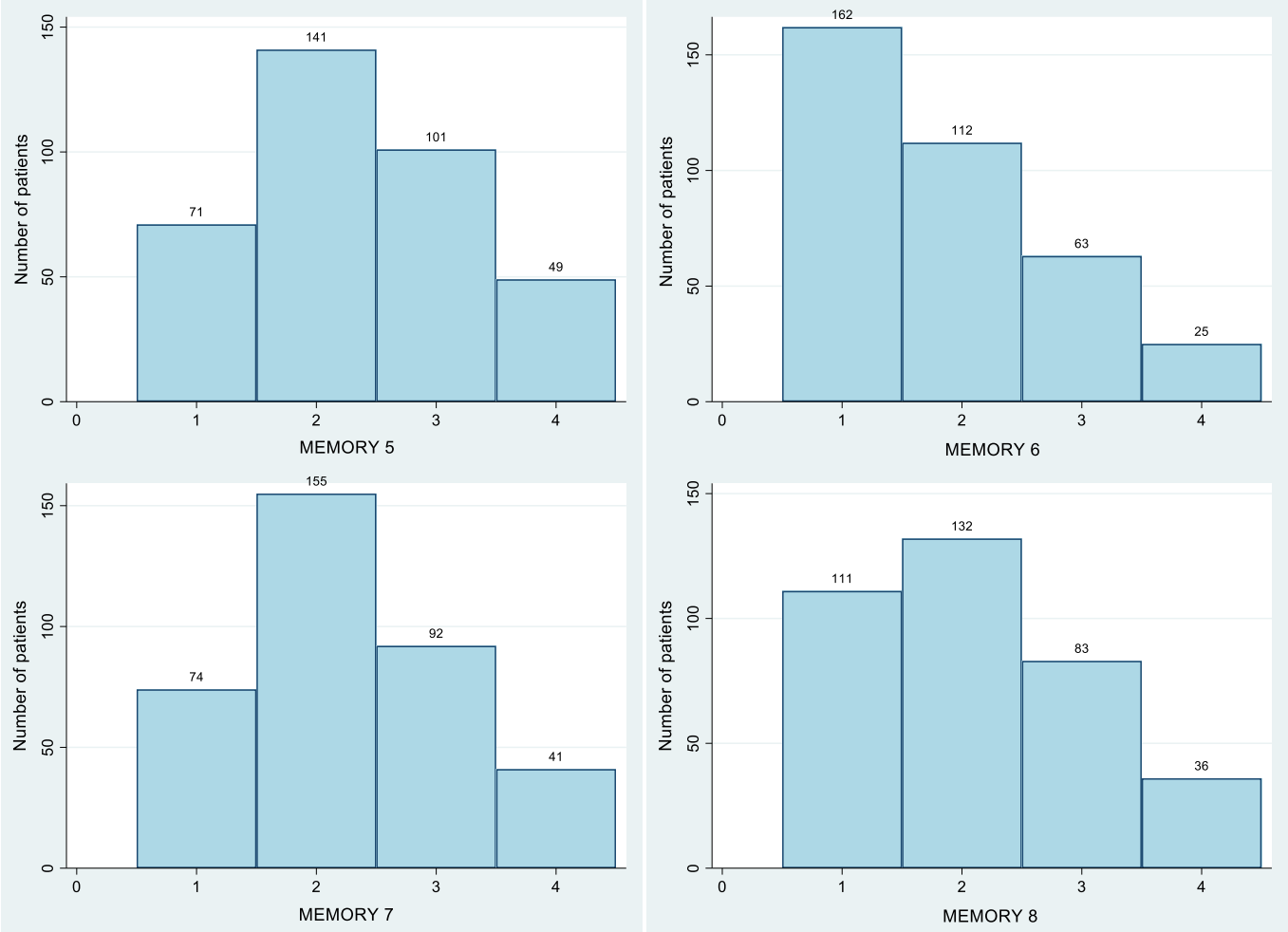

Figure 31: Patients' scores based on each MEMORY subdomain.

5.15. Regression analysis with MEMORY sum score

The linear regression of the "continuous" MEMORY sum score in the relevant sample of MCI patients showed a significant contribution of age at PET (p=0.012, β=-0.152) and ADAS13 score (p=0.005, β=0.168), but not the remaining predictor variables. The stepwise regression left also age at PET (p=0.022) and ADAS13 score (p=0.000) (table 2).

Table 2: Regression analysis based on the "continuous" MEMORY sum score of included MCI patients. All predictor variables were entered in the model. (*p:* significance, β standardized regression coefficient).

MEMORY sum score	**Linear regression analysis**		**Stepwise regression analysis**
	F= 2.26 p= 0.023 Adjusted R^2=0.027		F= 7.46 p= 0.0007 Adjusted R^2= 0.035
	p	β	*p*
BA 28 FDG uptake	0.921	.009	■
BA 28 Grey matter volume	0.485	.073	■
BA 34 FDG uptake	0.654	-.035	■
BA 34 Grey matter volume	0.150	-.148	■
Age at PET	**0.012**	-.152	**0.022**
Educational level (years)	0.947	.004	■
ADAS13 score	**0.005**	.168	**0.000**
APOE4 profile (binary)	0.654	.024	■

5.16. LANGUAGE sum score

Patients who have not answered on all questions of LANGUAGE domain of ECog were 12 (n=3 for LANGUAGE 2; n=2 for LANGUAGE 3; n=1 for LANGUAGE 4; n=3 for LANGUAGE 5; n=1 for LANGUAGE 6; n=1 for LANGUAGE 7; and n=1 for LANGUAGE 8).

Only 367 patients had complete LANGUAGE scores in all subdomains (figure 33). Adding all LANGUAGE subscores pro patient then subtracting nine allowed obtaining the LANGUAGE sum score for each patient. The scores ranged from zero to twenty-six (figure 34).

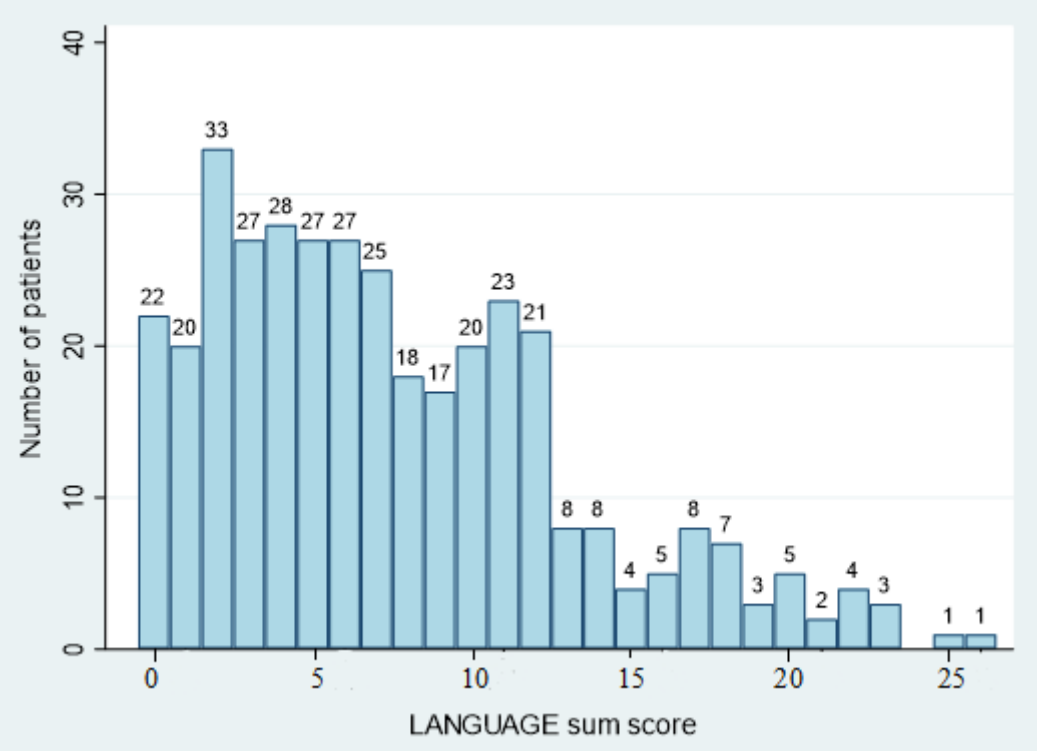

Figure 34: LANGUAGE sum score distribution in MCI study patients.

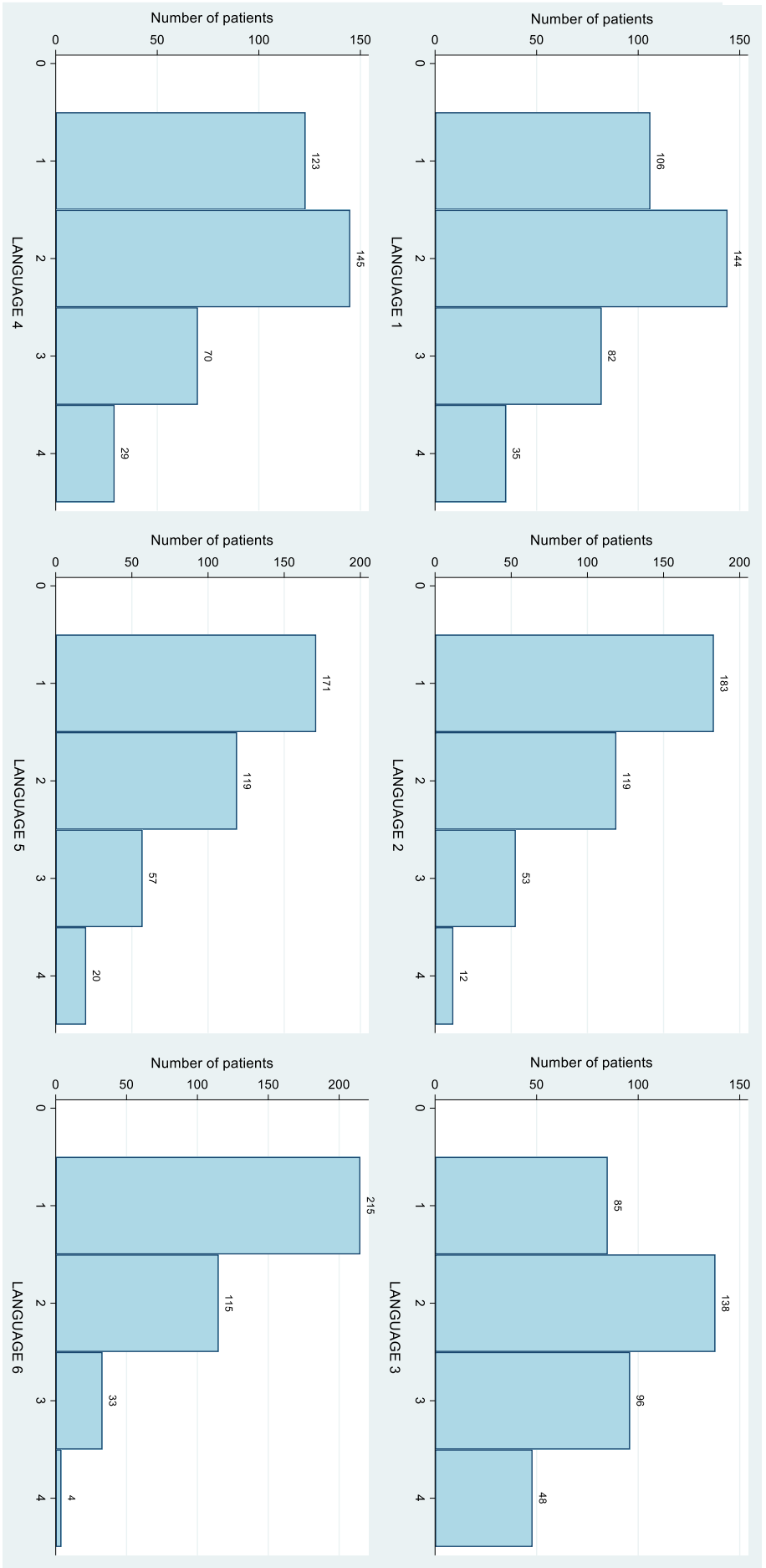
Number of patients
0
50
100
150
LANGUAGE 1
106
144
82
35
Number of patients
0
50
100
150
LANGUAGE 4
123
145
70
29
Number of patients
0
50
100
150
200
LANGUAGE 2
183
119
53
12
Number of patients
0
50
100
150
200
LANGUAGE 5
171
119
57
20
Number of patients
0
50
100
150
LANGUAGE 3
85
138
96
48
Number of patients
0
50
100
150
200
LANGUAGE 6
215
115
33
4

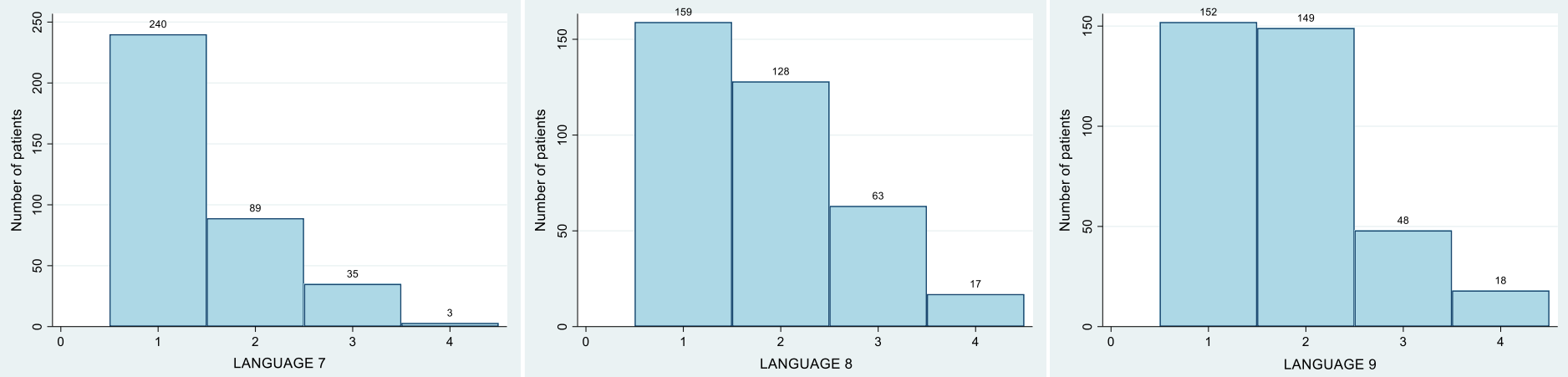

Figure 33: Patients' scores based on each LANGUAGE subdomain.

5.17. Regression analysis with LANGUAGE sum score

The regression analysis based on the “continuous” LANGUAGE sum score of relevant MCI patients showed no significant contribution of the predictor variables (table 3).

Table 3: Regression analysis based on the “continuous” LANGUAGE sum score of MCI patients. All predictor variables were entered in the model. (*p:* significance, β standardized regression coefficient).

LANGUAGE sum score	**Linear regression analysis**		**Stepwise regression analysis**
	F=1.44 *p*=0.180 Adjusted R^2=0.009		■
	p	β	*p*
BA 28 FDG uptake	0.128	0.132	■
BA 28 Grey matter volume	0.163	0.144	■
BA 34 FDG uptake	0.419	-0.063	■
BA 34 Grey matter volume	0.082	-0.178	■
Age at PET	0.585	0.034	■
Educational level (years)	0.092	-0.090	■
ADAS13 score	0.204	0.076	■
APOE4 profile (binary)	0.452	-0.040	■

5.18. Multivariate and univariate analyses with "continuous" VISSPAT sum score

- **BA 34**

A MANOVA analysis of BA 34 FDGu and GMV, both combined as dependent variables, was performed. The covariates were APOE4 carrier profile, "continuous" VISSPAT sum score, age at PET, educational level (years), and ADAS13 score. A two-way interaction between APOE4 carrier profile and "continuous" VISSPAT sum score was added to the model.

There was a statistical significance in the multivariate analysis regarding the effect of "continuous" VISSPAT sum score on BA 34 FDGu and GMV combined (p=0.043). The effect of APOE4 carrier profile on one side, and APOE4 carrier profile in two-way interaction with VISSPAT sum score on the other side, showed both no significant effect on BA 34 (p=0.851 and p=0.241, respectively).

Nevertheless, age at PET, educational level, and ADAS13 score showed statistical significance in the multivariate analysis on BA 34 FDGu and GMV (p=0.000, p=0.029, and p=0.000, respectively).

The univariate analysis ANOVA showed a significant effect of "continuous" VISSPAT sum score on BA 34 GMV (p=0.015), but not on BA 34 FDGu (p=0.750). Age at PET and ADAS 13 score showed a statistical significance on BA 34 GMV (both p=0.000), while only ADAS13 score and educational level had a significant effect on BA 34 FDGu (p=0.027 and p=0.003, respectively) based on ANOVA analysis. The results are summarized in table 4.

Table 4: Multivariate analysis (MANOVA) of BA 34 Grey matter volume and FDG uptake combined as dependent variables and univariate analysis (ANOVA) of BA 34 Grey matter volume, on one side, and BA 34 FDG uptake, on the other side, with APOE4 carrier profile, "continuous" VISSPAT sum score, age at PET, educational level, and ADAS13 score, as covariate. A two-way interaction between APOE4 carrier profile and "continuous" VISSPAT sum score was added to the model.

	MANOVA		**ANOVA**			
	BA 34 Grey matter volume * BA 34 FDG uptake		BA 34 Grey matter volume		BA 34 FDG uptake	
	F	*p*	F	*p*	F	*p*
"continuous" VISSPAT sum score	3.18	**0.043**	6.01	**0.015**	0.10	0.750
APOE4 profile (binary)	0.16	0.851	0.29	0.590	0.06	0.811
VISSPAT sum score * APOE4 profile (binary)	1.43	0.241	0.17	0.68	2.82	0.094
Age at PET	41.46	**0.000**	83.13	**0.000**	0.97	0.326
Educational level (years)	3.58	**0.029**	3.03	0.083	4.94	**0.027**
ADAS13 score	15.53	**0.000**	25.06	**0.000**	9.16	**0.003**

- **BA 28**

I performed a multivariate analysis (MANOVA) of BA 28 GMV and FDGu combined as dependent variables and univariate analysis (ANOVA) of BA 28 GMV, on one side, and BA28 FDGu, on the other side, with APOE4 carrier profile, “continuous” VISSPAT sum score, age at PET, educational level (years), and ADAS13 score, as covariate. A two-way interaction between APOE4 carrier profile and “continuous” VISSPAT sum score was added to the model.

There was no statistical significance regarding the effect of “continuous” VISSPAT sum score on BA 28 GMV and FDGu. Age at PET and ADAS13 score showed highly significant results in all tests ($p<0.001$). The educational level showed borderline significant impact on BA 28 in the multivariate and univariate analysis.

The results are summarized in Table 5.

Table 5: Multivariate analysis (MANOVA) of BA 28 Grey matter volume and FDG uptake combined as dependent variables and univariate analysis (ANOVA) of BA 28 Grey matter volume, on one side, and BA 28 FDG uptake, on the other side, with APOE4 carrier profile, "continuous" VISSPAT sum score, age at PET, educational level (years), and ADAS13 score, as covariate. A two-way interaction between APOE4 carrier profile and "continuous" VISSPAT sum score was added to the model.

	MANOVA		**ANOVA**			
	BA 28 Grey matter volume * BA 28 FDG uptake		BA 28 Grey matter volume		BA 28 FDG uptake	
	F	*p*	F	*p*	F	*p*
"continuous" VISSPAT sum score	1.99	0.138	1.91	0.167	0.88	0.350
APOE4 profile (binary)	1.93	0.147	3.60	0.059	0.01	0.913
VISSPAT sum score * APOE4 profile (binary)	2.55	0.079	3.42	0.065	3.30	0.070
Age at PET	30.97	**0.000**	60.85	**0.000**	12.35	**0.001**
Educational level (years)	2.94	**0.054**	4.08	**0.044**	3.67	**0.0561**
ADAS13 score	24.90	**0.000**	34.36	**0.000**	31.21	**0.0000**

5.19. Multivariate and univariate analyses with continuous SP-VISSPAT sum score

I also performed a multivariate analysis (MANOVA) of BA 34 GMV and FDGu combined as dependent variables and univariate analysis (ANOVA) of BA 34 GMV, on one side, and BA 34 FDGu, on the other side, with APOE4 carrier profile, “continuous” SP-VISSPAT sum score, age at PET, years of education, and ADAS13 score, as covariate. A two-way interaction between APOE4 carrier profile and “continuous” SP-VISSPAT sum score was added to the model.

There was no statistical significance neither in the multivariate analysis regarding the effect of SP-VISSPAT sum score on BA 34 FDGu uptake and GMV combined, nor in the univariate analysis.

Nevertheless, age, and ADAS13 score showed strong statistical significance in the multivariate analysis on BA 34 FDGu and GMV and in the univariate analysis regarding BA 34 GMV (p=0.000, both). Only ADAS13 score showed significant results in the univeriate analysis based on BA 34 FDGu (p=0.005).

The results are summarized in table 6.

Table 6: Multivariate analysis (MANOVA) of BA 34 Grey matter volume and FDG uptake combined as dependent variables and univariate analysis (ANOVA) of BA 34 Grey matter volume, on one side, and BA 34 FDG uptake, on the other side, with APOE4 carrier profile, "continuous" SP-VISSPAT sum score, age at PET, educational level (years), and ADAS13 score, as covariate. A two-way interaction between APOE4 carrier profile and "continuous" SP-VISSPAT sum score was added to the model.

	MANOVA		**ANOVA**			
	BA 34 Grey matter volume * BA 34 FDG uptake		BA 34 Grey matter volume		BA 34 FDG uptake	
	F	*p*	F	*p*	F	*p*
"continuous" **SP**-VISSPAT sum score	0.02	0.983	0.03	0.867	0.01	0.917
APOE4 profile (binary)	0.19	0.830	0.36	0.549	0.04	0.846
"continuous" SP-VISSPAT sum score * APOE4 profile (binary)	1.83	0.162	0.11	0.744	3.37	0.067
Age at PET	24.36	**0.000**	48.75	**0.000**	1.48	0.225
Educational level (years)	2.12	0.122	1.28	0.259	3.42	0.065
ADAS13 score	15.86	**0.000**	26.72	**0.000**	8.21	**0.005**

6. Discussion of results

The main outcome of this study was the significant correlation between the neurodegeneration in the medial part of the ERC (BA 34) and an impaired performance in the spatial navigation over a span of 10 years. (1)

These findings were retained owing to a significant reduced GMV in BA 34 in MCI patients who, based on a higher “continuous” VISSPAT sum score, presented an alteration in their spatial navigation and spatial memory, in contrast with patients without alteration in their navigation performance. Moreover, GMV in BA 34 had a significant negative contribution in the regression of the VISSPAT sum score. (1) These findings were not observed with scores related to memory or language. Additionally, the findings related to spatial orientation as reported by study-partner were not significant, which shows that the self-awareness of spatial orientation and navigation skills in MCI patients is more accurate with the anatomical changes in ERC in general and BA 34 specifically. Further, there was no significant association between GMV in the lateral part of ERC (BA 28) and VISSPAT sum score in MCI patients. Despite studying different co-factors related to aging and cognition, the neurodegeneration traduced by a volume loss in BA 34 was significantly correlated with an alteration in the spatial navigation. This suggests that spatial navigation and spatial memory are particularly sensitive to neurodegeneration in BA 34, rather than BA 28. (1)

On the other hand, the study hypothesis suggesting that reduced FDGu in BA 34 could be an independent predictor of impairment in spatial navigation or spatial memory performance could not be validated. In regression analysis, FDGu in BA 34 showed no significant correlation with the VISSPAT sum score. (1) The latter hypothesis was based on the fact that synaptic dysfunction generally precedes cell

death. (57) It is therefore possible, that some patients with MCI might present reduction in FDG uptake simultaneously with preserved GMV in BA 34. Error amplification related to partial volume correction used in PET investigations might have lead to an increased inter-subject disparity, and also might be an additional explanation of discordance between VISSPAT sum score and FDGu in BA 34. (1, 58)

A further finding of this study was the age-related spatial navigation performance and spatial memory in MCI patients. The spatial navigation might be more strongly impaired in younger MCI patients. (1) This interpretation is retained from the negative sign of the age coefficient in the VISSPAT sum score regression model. (1)

Moreover, with the same level of overall cognitive impairment and the similar amount of BA 34 atrophy, the spatial orientation in younger MCI patients is more highly impaired than in older MCI patients, based on the results of the regression analysis. (1) In absolute terms, spatial navigation performance showed no discrepancy between older and younger MCI patients. (1) This could be explained to some extent by the fact that the cognitive profiles and the processing of spatial navigation between younger and older MCI patients are different.

Several previous studies reported the impact of aging on alteration of spatial navigation, and thus as independent factor of performance decline. The study of Lithfous and co-workers distinguished between allocentric and egocentric orientation performance in relation with aging. (59) The egocentric coding of spatial orientation is self-centred, whereas the allocentric orientation is object-centred and requires preserved attention and perception and depends on the executive function of the person. While the egocentric orientation was less affected in elderly patients, the allocentric coding showed an age-related decline in the same population. (59) The

VISSPAT items, on which our study was based, are related to spatial orientation in everyday's life and therefore, in contrary to experimental studies, no differentiation had been made between the two aspects of spatial orientation. (1)

Moffat and collaborators showed during virtual environment navigation lower activation in the hippocampus, medial parietal lobe, parahippocampal gyrus, and retrosplenial cortex in elderly patients when compared to younger controls. Moreover, the older participants presented higher activation in medial frontal lobe and anterior cingulate gyrus. (60) Similarly, Irving and collaborators showed through FDG-PET findings in their patients a decreased navigation-induced regional cerebral glucose metabolism in precuneus and hippocampus in relation to advanced age, while in the same patients, regional cerebral glucose metabolism in the cerebellum, frontal cortex, and basal ganglia increased compared to younger controls. (61) This suggests age-dependent differences in spatial memory and navigation skills, in addition to differences in the coding process and in relevant anatomical structures.

Similarly to aging, in some psychiatric pathology as the anorexia nervosa, where there is a decrease in somatosensory inputs in relation to body mass loss, impairment of spatial orientation was observed. This impairment affects essentially visual, tactile, and gravitational information in the parietal cortex, which also seems to have a role in the allocentric spatial orientation. (62)

Sherrill and collaborators (63) showed in healthy young adults that participants, who were more successful in updating orientation and position during first person-perspective goal-directed navigation in the absence of landmarks, had greater GMV in following navigation-related cerebral regions: right ERC, in addition to hippocampus and thalamus, both bilaterally. Moreover, the results of Sherrill and collaborators showed that the GMV difference in the ERC was located in the

posterior region of the ERC, which confirms what has already been described by other authors who reported that the medial ERC with its posterior connections (BA 34) is the human homolog to the medial ERC in rodents. (12, 35)

In this study, each participant was used at its own control over a span of 10 years. Sex was, therefore, not included as covariant. (1) Thus, different studies have shown differences in the orientation profile and spatial navigation performance between male and female participants. Anatomically, FDG-PET in women showed an increase of regional cerebral glucose metabolism in the right middle temporal gyrus and the left hippocampus, while men in the superior vermis. (61)

Although previous studies showed that grid cells are presented with lower density in ERC of APOE4 carriers, and that affected subjects are at higher risk of presenting with an alteration in their spatial navigation performance years before any cognitive impairment could be detected, (64) the current study revealed no significant correlation between BA 34 GMV and navigation performance or spatial memory on one hand and APOE4-positivity on the other hand. (1)

Since being a carrier of APOE4 allele is a risk factor for evolution from MCI to Alzheimer's disease, the findings of this study would suggest that the correlation between ERC degeneration and impaired spatial navigation is not a characteristic aspect of Alzheimer's disease. (1) In fact, various other neurodegenerative pathologies, such as argyrophilic grain disease, limbic-predominant age-related TDP-43 encephalopathy, primary age-related tauopathy, might alter the functional and structural integrity in ERC and lead to MCI, (65, 66) especially MCI phenotypes with pronounced deficits in navigation performance and spatial orientation. (67, 68)

7. Clinical implications

This study showed that VISSPAT subdomain of ECog includes items, which could be used as a screening method to detect anatomical changes in the BA 34 at MCI stage. (1) However, as reported in the manuscript, other factors such as age, overall cognition (ADAS13 score) and total intracranial volume were better predictors and should be taken into account. (1) In the published data, VISSPAT sum score explained only 0.4% of the changes of BA 34 GMV and therefore, could only weakly predict BA 34 degeneration in MCI patients. (1)

Nevertheless, training spatial orientation could be used as a rehabilitation tool in order to optimize the spatial memory and the functional connections of the ERC. Peng and collaborators showed the positive impact of long-term navigation experience in taxi drivers on their spatial orientation and on the connectivity patterns of the ERC. (69) Verbally-guided passive navigation in virtual reality training programs has been tested in patients with impaired spatial orientation due to focal brain lesions in relation to stroke. Over five training sessions, participants recalled different routes in a virtual place. In term of this experiment, both orientation-impaired patients and healthy controls showed a significant improvement in spatial navigation performance. (70) Improving the spatial memory could also have a positive impact on other types of declarative memory. Caglio and collaborators reported an experiment where virtual navigation through 3D video games was performed in a 24-year-old man with a traumatic brain injury and showed an improvement of memory function correlated with an increase of the activation of the hippocampal and para-hippocampal brain regions on fMRI. (71)

The integrity of the cells functioning in ERC does not only play a role in spatial navigation but also on the behavior of the person in relation to its environment.

Experiments in rats showed that the consistent and proper functioning in GC and head direction cells predicts in 70% of cases the movement option in the rodent and adequate behavioral choices in relation to this finding. This was not the case when the cells did not show a stable consistent readout. (72)

Therefore, navigation trainings might be proposed to optimize the functional organization of ERC as a part of the non-pharmacological management of patients with high-risk of MCI, if screened at early stages.

8. Limitations

The first limitation of this study is related to including a specific population with MCI without comparing with healthy subjects. Moreover, the retrospective aspect of data collection to assess visuospatial performance during daily life activity is a further limitation.

Even though we observed significant correlations between BA 34 and spatial navigation, allowing us replication of findings obtained from animal experiments, we should not omit to mention that spatial navigation in humans is a very complex function. As an example, the horizontal navigation in humans relays more on visual inputs, while the vestibular multisensory cortex seems more relevant for the vertical navigation. (73) This demonstrates, among others, the importance of visual inputs in spatial cells in humans compared to rodents, which is more based on tactile and olfactory functions.

The allocentric spatial orientation was early shown to be related to the right temporal lobe. In patients with unilateral temporal lobectomy, the long-term allocentric spatial memories were despaired only when the right side was affected. (74) Thus, our study was based on the BA 34 GMV in both sides, which presents another limitation.

Moreover, we have not explored changes in other brain regions, which might play a role in the spatial navigation and memory, e.g. PRC and PHC (which are critical for landmark recognition), (75) retrosplenial cortex (which is involved in localization and orientation through the translation of egocentriccally experienced visual flow into an allocentric model of position and movement (76)), retrosplenial and medial parietal lobe regions (which support long-term spatial knowledge) (77) and the anterior and lateral thalamic regions, which also are reported to play a role in the spatial mapping and memory. (78)

9. Conclusions

This study provides lesion-based evidence that BA 34 integrity is specifically associated with spatial navigation. Nevertheless, due to the multifactorial aspect of the spatial navigation on one hand, and the brain morphology in ERC on the other hand, the results cannot be used in everyday practice, and the predictive value of MRI in exploring the integrity of ERC in relation to spatial orientation is only weak. (1)

10. References

1. Hallab A, Lange C, Apostolova I, Özden C, Gonzalez-Escamilla G, Klutmann S, Brenner W, Grothe MJ, Buchert, R. Impairment of Everyday Spatial Navigation Abilities in Mild Cognitive Impairment Is Weakly Associated with Reduced Grey Matter Volume in the Medial Part of the Entorhinal Cortex. Journal of Alzheimer's disease : JAD. 2020;78(3):1149-59.

2. Canto CB, Wouterlood FG, Witter MP. What does the anatomical organization of the entorhinal cortex tell us? Neural plasticity. 2008;2008:381243.

3. Eifuku S. [Brodmann Areas 27, 28, 36 and 37: The Parahippocampal and the Fusiform Gyri]. Brain and nerve = Shinkei kenkyu no shinpo. 2017;69(4):439-51.

4. Kobayashi Y. [Spatial Cognition and Episodic Memory Formation in the Limbic Cortex]. Brain and nerve = Shinkei kenkyu no shinpo. 2017;69(4):427-37.

5. Brodmann. Vergleichende Lokalisationslehre der Grosshirnrinde in ihren Prinzipien dargestellt auf Grund des Zellenbaues. 1909.

6. Hafting T, Fyhn M, Molden S, Moser MB, Moser EI. Microstructure of a spatial map in the entorhinal cortex. Nature. 2005;436(7052):801-6.

7. Sargolini F, Fyhn M, Hafting T, McNaughton BL, Witter MP, Moser MB, Moser EI. Conjunctive representation of position, direction, and velocity in entorhinal cortex. Science (New York, NY). 2006;312(5774):758-62.

8. Tsao A, Sugar J, Lu L, Wang C, Knierim JJ, Moser MB, Moser EI. Integrating time from experience in the lateral entorhinal cortex. Nature. 2018;561(7721):57-62.

9. Habets AM, Lopes Da Silva FH, Mollevanger WJ. An olfactory input to the hippocampus of the cat: field potential analysis. Brain research. 1980;182(1):47-64.

10. Kerr KM, Agster KL, Furtak SC, Burwell RD. Functional neuroanatomy of the parahippocampal region: the lateral and medial entorhinal areas. Hippocampus. 2007;17(9):697-708.

11. Deshmukh SS, Knierim JJ. Representation of non-spatial and spatial information in the lateral entorhinal cortex. Frontiers in behavioral neuroscience. 2011;5:69.

12. Navarro Schroder T, Haak KV, Zaragoza Jimenez NI, Beckmann CF, Doeller CF. Functional topography of the human entorhinal cortex. eLife. 2015;4.

13. Vilberg KL, Davachi L. Perirhinal-hippocampal connectivity during reactivation is a marker for object-based memory consolidation. Neuron. 2013;79(6):1232-42.

14. Staresina BP, Duncan KD, Davachi L. Perirhinal and parahippocampal cortices differentially contribute to later recollection of object- and scene-related event details. The Journal of neuroscience : the official journal of the Society for Neuroscience. 2011;31(24):8739-47.

15. Stephen Walter Ranson WBS. Anatomy of the Nervous System1920.

16. Wikipedia. Brodmann area 2021 [Available from: https://en.wikipedia.org/wiki/Brodmann_area. Accessed on 24.10.21]

17. O'Keefe J, Dostrovsky J. The hippocampus as a spatial map. Preliminary evidence from unit activity in the freely-moving rat. Brain research. 1971;34(1):171-5.

18. Kjelstrup KB, Solstad T, Brun VH, Hafting T, Leutgeb S, Witter MP, Moser EI, Moser MB. Finite scale of spatial representation in the hippocampus. Science (New York, NY). 2008;321(5885):140-3.

19. Anderson MI, Jeffery KJ. Heterogeneous modulation of place cell firing by changes in context. The Journal of neuroscience : the official journal of the Society for Neuroscience. 2003;23(26):8827-35.

20. Taube JS, Muller RU, Ranck JB, Jr. Head-direction cells recorded from the postsubiculum in freely moving rats. I. Description and quantitative analysis. The Journal of neuroscience : the official journal of the Society for Neuroscience. 1990;10(2):420-35.

21. Taube JS. The head direction signal: origins and sensory-motor integration. Annual review of neuroscience. 2007;30:181-207.

22. Boccara CN, Sargolini F, Thoresen VH, Solstad T, Witter MP, Moser EI, Moser EI. Grid cells in pre- and parasubiculum. Nature neuroscience. 2010;13(8):987-94.

23. Krupic J, Burgess N, O'Keefe J. Neural representations of location composed of spatially periodic bands. Science (New York, NY). 2012;337(6096):853-7.

24. Barry C, Ginzberg LL, O'Keefe J, Burgess N. Grid cell firing patterns signal environmental novelty by expansion. Proceedings of the National Academy of Sciences of the United States of America. 2012;109(43):17687-92.

25. Fyhn M, Hafting T, Witter MP, Moser EI, Moser MB. Grid cells in mice. Hippocampus. 2008;18(12):1230-8.

26. Lever C, Burton S, Jeewajee A, O'Keefe J, Burgess N. Boundary vector cells in the subiculum of the hippocampal formation. The Journal of neuroscience : the official journal of the Society for Neuroscience. 2009;29(31):9771-7.

27. Savelli F, Yoganarasimha D, Knierim JJ. Influence of boundary removal on the spatial representations of the medial entorhinal cortex. Hippocampus. 2008;18(12):1270-82.

28. Stewart S, Jeewajee A, Wills TJ, Burgess N, Lever C. Boundary coding in the rat subiculum. Philosophical transactions of the Royal Society of London Series B, Biological sciences. 2014;369(1635):20120514.

29. Tsao A, Moser MB, Moser EI. Traces of experience in the lateral entorhinal cortex. Current biology : CB. 2013;23(5):399-405.

30. Hoydal OA, Skytoen ER, Andersson SO, Moser MB, Moser EI. Object-vector coding in the medial entorhinal cortex. Nature. 2019;568(7752):400-4.

31. Sarel A, Finkelstein A, Las L, Ulanovsky N. Vectorial representation of spatial goals in the hippocampus of bats. Science (New York, NY). 2017;355(6321):176-80.

32. McNaughton BL, Knierim JJ, Wilson MA. Vector encoding and the vestibular foundations of spatial cognition: Neurophysiological and computational mechanisms. The cognitive neurosciences. Cambridge, MA, US: The MIT Press; 1995. p. 585-95.

33. Watrous AJ, Miller J, Qasim SE, Fried I, Jacobs J. Phase-tuned neuronal firing encodes human contextual representations for navigational goals. eLife. 2018;7.

34. Doeller CF, Barry C, Burgess N. Evidence for grid cells in a human memory network. Nature. 2010;463(7281):657-61.

35. Maass A, Berron D, Libby LA, Ranganath C, Duzel E. Functional subregions of the human entorhinal cortex. eLife. 2015;4.

36. Nadasdy Z, Nguyen TP, Torok A, Shen JY, Briggs DE, Modur PN, Buchanan RJ. Context-dependent spatially periodic activity in the human entorhinal cortex. Proceedings of the National Academy of Sciences of the United States of America. 2017;114(17):E3516-e25.

37. Dieterich M, Brandt T. Global orientation in space and the lateralization of brain functions. Current opinion in neurology. 2018;31(1):96-104.

38. Constantinescu AO, O'Reilly JX, Behrens TEJ. Organizing conceptual knowledge in humans with a gridlike code. Science (New York, NY). 2016;352(6292):1464-8.

39. Braak H, Braak E. On areas of transition between entorhinal allocortex and temporal isocortex in the human brain. Normal morphology and lamina-specific pathology in Alzheimer's disease. Acta neuropathologica. 1985;68(4):325-32.

40. Chen Y, Liu L, Li M, Yao E, Hao J, Dong Y, Zheng X, Liu X. Expression of human Tau40 in the medial entorhinal cortex impairs synaptic plasticity and associated cognitive functions in mice. Biochemical and biophysical research communications. 2018;496(3):1006-12.

41. Amoroso N, Rocca M, Bellotti R, Fanizzi A, Monaco A, Tangaro S. Alzheimer's disease diagnosis based on the Hippocampal Unified Multi-Atlas Network (HUMAN) algorithm. Biomedical engineering online. 2018;17(1):6.

42. Sarica A, Vasta R, Novellino F, Vaccaro MG, Cerasa A, Quattrone A. MRI Asymmetry Index of Hippocampal Subfields Increases Through the Continuum From the Mild Cognitive Impairment to the Alzheimer's Disease. Frontiers in neuroscience. 2018;12:576.

43. Khan UA, Liu L, Provenzano FA, Berman DE, Profaci CP, Sloan R, Mayeux R, Duff K, Small SA. Molecular drivers and cortical spread of lateral entorhinal cortex dysfunction in preclinical Alzheimer's disease. Nature neuroscience. 2014;17(2):304-11.

44. Thaker AA, Weinberg BD, Dillon WP, Hess CP, Cabral HJ, Fleischman DA, Leurgans SE, Bennett DA, Hyman BT, Albert MS, Killiany RJ, Fishl B, Dale AM, Desikan RS. Entorhinal Cortex: Antemortem Cortical Thickness and Postmortem Neurofibrillary Tangles and Amyloid Pathology. AJNR American journal of neuroradiology. 2017;38(5):961-5.

45. WHO. The top 10 causes of death. 2020 [Available from: https://www.who.int/en/news-room/fact-sheets/detail/the-top-10-causes-of-death. Accessed on 24.10.21]

46. WHO. Towards a dementia plan: a WHO guide. 2021 [Available from: https://www.who.int/mental_health/neurology/dementia/en/. Accessed on 24.10.21]

47. Hadjichrysanthou C, McRae-McKee K, Evans S, de Wolf F, Anderson RM. Potential Factors Associated with Cognitive Improvement of Individuals Diagnosed with Mild Cognitive Impairment or Dementia in Longitudinal Studies. Journal of Alzheimer's disease : JAD. 2018;66(2):587-600.

48. ADNI. ADNI official Website. 2021 [Available from: http://adni.loni.usc.edu/. Accessed on 24.10.21]

49. Farias ST, Mungas D, Reed BR, Cahn-Weiner D, Jagust W, Baynes K, Decarli C. The measurement of everyday cognition (ECog): scale development and psychometric properties. Neuropsychology. 2008;22(4):531-44.

50. Lange C, Suppa P, Frings L, Brenner W, Spies L, Buchert R. Optimization of Statistical Single Subject Analysis of Brain FDG PET for the Prognosis of Mild Cognitive Impairment-to-Alzheimer's Disease Conversion. J Alzheimers Dis. 2016;49(4):945-59.

51. Andersson JL, Vagnhammar BE, Schneider H. Accurate attenuation correction despite movement during PET imaging. J Nucl Med. 1995;36(4):670-8.

52. Gonzalez-Escamilla G, Lange C, Teipel S, Buchert R, Grothe MJ, Alzheimer's Disease Neuroimaging I. PETPVE12: an SPM toolbox for Partial Volume Effects correction in brain PET - Application to amyloid imaging with AV45-PET. Neuroimage. 2017;147:669-77.

53. Minoshima S, Frey KA, Foster NL, Kuhl DE. Preserved pontine glucose metabolism in Alzheimer disease: a reference region for functional brain image (PET) analysis. J Comput Assist Tomogr. 1995;19(4):541-7.

54. Ashburner J, Friston KJ. Unified segmentation. Neuroimage. 2005;26(3):839-51.

55. Herron TJ, Kang XJ, Woods DL. Automated measurement of the human corpus callosum using MRI. Front Neuroinform. 2012;6.

56. Maguire EA, Burgess N, O'Keefe J. Human spatial navigation: cognitive maps, sexual dimorphism, and neural substrates. Curr Opin Neurobiol. 1999;9(2):171-7.

57. Selkoe DJ. Alzheimer's disease is a synaptic failure. Science (New York, NY). 2002;298(5594):789-91.

58. Erlandsson K, Buvat I, Pretorius PH, Thomas BA, Hutton BF. A review of partial volume correction techniques for emission tomography and their applications in neurology, cardiology and oncology. Phys Med Biol. 2012;57(21):R119-59.

59. Lithfous S, Dufour A, Blanc F, Despres O. Allocentric but not egocentric orientation is impaired during normal aging: an ERP study. Neuropsychology. 2014;28(5):761-71.

60. Moffat SD, Elkins W, Resnick SM. Age differences in the neural systems supporting human allocentric spatial navigation. Neurobiology of aging. 2006;27(7):965-72.

61. Irving S, Schoberl F, Pradhan C, Brendel M, Bartenstein P, Dieterich M, Brandt T, Zwergal A. A novel real-space navigation paradigm reveals age- and gender-dependent changes of navigational strategies and hippocampal activation. Journal of neurology. 2018;265(Suppl 1):113-26.

62. Guardia D, Carey A, Cottencin O, Thomas P, Luyat M. Disruption of spatial task performance in anorexia nervosa. PloS one. 2013;8(1):e54928.

63. Sherrill KR, Chrastil ER, Aselcioglu I, Hasselmo ME, Stern CE. Structural Differences in Hippocampal and Entorhinal Gray Matter Volume Support Individual Differences in First Person Navigational Ability. Neuroscience. 2018;380:123-31.

64. Kunz L, Schroder TN, Lee H, Montag C, Lachmann B, Sariyska R, Reuter M, Stirnberg R, Stöcker T, Massing-Floeter PC, Fell J, Doeller CF, Axmacher N. Reduced grid-cell-like representations in adults at genetic risk for Alzheimer's disease. Science (New York, NY). 2015;350(6259):430-3.

65. Abner EL, Kryscio RJ, Schmitt FA, Fardo DW, Moga DC, Ighodaro ET, Jicha GA, Yu L, Dodge HH, Xiong C, Woltjer RL, Schneider JA, Cairns N, Bennett D, Neslon PT. Outcomes after diagnosis of mild cognitive impairment in a large autopsy series. Ann Neurol. 2017;81(4):549-59.

66. Nelson PT, Dickson DW, Trojanowski JQ, Jack CR, Boyle PA, Arfanakis K, Rademakers R, Alafuzoff I, Attems J, Brayne C, Coyle-Gilchrist ITS, Chui HC, Fardo DW, Flanagan ME, Halliday G, Hokkanen SRK, Hunter S, Jicha GA, Katsumata Y, Kawas CH, Keene CD, Kovacs GG, Kukull WA, Levey AI, Makkinejad N, Montine TJ, Murayama S, Murray ME, Nag S, Rissman RA, Seeley WW, Sperling RA, Lii CLW, Yu L, Schneider JA. Limbic-predominant age-related TDP-43 encephalopathy (LATE): consensus working group report. Brain. 2019;142(6):1503-27.

67. Howett D, Castegnaro A, Krzywicka K, Hagman J, Marchment D, Henson R, Rio M, King JA, Burgess N, Chan D. Differentiation of mild cognitive impairment using an entorhinal cortex-based test of virtual reality navigation. Brain. 2019;142:1751-66.

68. Stangl M, Achtzehn J, Huber K, Dietrich C, Tempelmann C, Wolbers T. Compromised Grid-Cell-like Representations in Old Age as a Key Mechanism to Explain Age-Related Navigational Deficits. Curr Biol. 2018;28(7):1108-+.

69. Peng L, Zeng LL, Liu Q, Wang L, Qin J, Xu H, Shen H, Li H, Hu D. Functional connectivity changes in the entorhinal cortex of taxi drivers. Brain and behavior. 2018;8(9):e01022.

70. Kober SE, Wood G, Hofer D, Kreuzig W, Kiefer M, Neuper C. Virtual reality in neurologic rehabilitation of spatial disorientation. Journal of neuroengineering and rehabilitation. 2013;10:17.

71. Caglio M, Latini-Corazzini L, D'Agata F, Cauda F, Sacco K, Monteverdi S, Zettin M, Duca S, Geminiani G. Virtual navigation for memory rehabilitation in a traumatic brain injured patient. Neurocase. 2012;18(2):123-31.

72. Weiss S, Talhami G, Gofman-Regev X, Rapoport S, Eilam D, Derdikman D. Consistency of Spatial Representations in Rat Entorhinal Cortex Predicts Performance in a Reorientation Task. Current biology : CB. 2017;27(23):3658-65.e4.

73. Zwergal A, Schoberl F, Xiong G, Pradhan C, Covic A, Werner P, Trapp C, Bartenstein P, La Fougère C, Jahn K, Dieterch M, Brandt T. Anisotropy of Human Horizontal and Vertical Navigation in Real Space: Behavioral and PET Correlates. Cerebral cortex (New York, NY : 1991). 2016;26(11):4392-404.

74. Feigenbaum JD, Morris RG. Allocentric versus egocentric spatial memory after unilateral temporal lobectomy in humans. Neuropsychology. 2004;18(3):462-72.

75. Zhang H, Copara M, Ekstrom AD. Differential recruitment of brain networks following route and cartographic map learning of spatial environments. PloS one. 2012;7(9):e44886.

76. Gramann K, Onton J, Riccobon D, Mueller HJ, Bardins S, Makeig S. Human brain dynamics accompanying use of egocentric and allocentric reference frames during navigation. Journal of cognitive neuroscience. 2010;22(12):2836-49.

77. Epstein RA, Vass LK. Neural systems for landmark-based wayfinding in humans. Philosophical transactions of the Royal Society of London Series B, Biological sciences. 2014;369(1635):20120533.

78. Clark BJ, Harvey RE. Do the anterior and lateral thalamic nuclei make distinct contributions to spatial representation and memory? Neurobiology of learning and memory. 2016;133:69-78.

VI- Author's contributions

Eidesstattliche Versicherung

„Ich, Asma Hallab, versichere an Eides statt durch meine eigenhändige Unterschrift, dass ich die vorgelegte Dissertation mit dem Thema: „Role of MRI and FDG-PET in the exploration of the Entorhinal Cortex in relation to spatial orientation in patients with mild cognitive impairment“ / „Bedeutung der MRT und FDG-PET in der Exploration des Entorhinalen Kortex im Zusammenhang mit der räumlichen Orientierung bei Patienten mit leichter kognitiver Beeinträchtigung“ selbstständig und ohne nicht offengelegte Hilfe Dritter verfasst und keine anderen als die angegebenen Quellen und Hilfsmittel genutzt habe.

Alle Stellen, die wörtlich oder dem Sinne nach auf Publikationen oder Vorträgen anderer Autoren/innen beruhen, sind als solche in korrekter Zitierung kenntlich gemacht. Die Abschnitte zu Methodik (insbesondere praktische Arbeiten, Laborbestimmungen, statistische Aufarbeitung) und Resultaten (insbesondere Abbildungen, Graphiken und Tabellen) werden von mir verantwortet.

Ich versichere ferner, dass ich die in Zusammenarbeit mit anderen Personen generierten Daten, Datenauswertungen und Schlussfolgerungen korrekt gekennzeichnet und meinen eigenen Beitrag sowie die Beiträge anderer Personen korrekt kenntlich gemacht habe (siehe Anteilserklärung). Texte oder Textteile, die gemeinsam mit anderen erstellt oder verwendet wurden, habe ich korrekt kenntlich gemacht.

Meine Anteile an etwaigen Publikationen zu dieser Dissertation entsprechen denen, die in der untenstehenden gemeinsamen Erklärung mit dem/der Erstbetreuer/in, angegeben sind. Für sämtliche im Rahmen der Dissertation entstandenen Publikationen wurden die Richtlinien des ICMJE (International Committee of Medical Journal Editors; www.icmje.og) zur Autorenschaft eingehalten. Ich erkläre ferner, dass ich mich zur Einhaltung der Satzung der Charité – Universitätsmedizin Berlin zur Sicherung Guter Wissenschaftlicher Praxis verpflichte.

Weiterhin versichere ich, dass ich diese Dissertation weder in gleicher noch in ähnlicher Form bereits an einer anderen Fakultät eingereicht habe.

Die Bedeutung dieser eidesstattlichen Versicherung und die strafrechtlichen Folgen einer unwahren eidesstattlichen Versicherung (§§156, 161 des Strafgesetzbuches) sind mir bekannt und bewusst.“

Datum Unterschrift

Anteilserklärung an den erfolgten Publikationen

Asma Hallab hatte folgenden Anteil an der folgenden Publikation:

Asma Hallab, Catharina Lange, Ivayla Apostolova, Cansu Özden, Gabriel Gonzalez-Escamilla, Susanne Klutmann, Winfried Brenner, Michel J. Grothe and Ralph Buchert ∗ for the Alzheimer's Disease Neuroimaging Initiative. Impairment of Everyday Spatial Navigation Abilities in Mild Cognitive Impairment Is Weakly Associated with Reduced Grey Matter Volume in the Medial Part of the Entorhinal Cortex. Journal of Alzheimer's Disease. 2020.

Beitrag im Einzelnen (bitte ausführlich ausführen):

Asma Hallab war für die Entwicklung der Fragestellung primär verantwortlich. Die Entwicklung des Studienkonzepts/-protokolls erfolgte gemeinsam mit den Betreuern. Für die neuroanatomischen und neuropsychologischen Grundlagen führte sie, neben ihrer Weiter-/Ausbildung, eine ausführliche Literaturrecherche durch, die sie in dieser Arbeit zusammengefasst hat.

Nach der Datengewinnung aus der ADNI Database und der technischen Bearbeitung der MRT und PVE Korrektur der PET Daten, die von den Ko-Autoren primär durchgeführt worden ist, war sie die Hauptverantwortliche für die Datenanalyse (Auswahlkriterien, Auswahl der biodemographischen Daten und Co-variablen, Selektion der relevanten neuropsychologischen Testungen, deren Interpretationen und Befunde), und für die Statistik. Im Hauptteil des Manuskripts, wurden die Tabellen 1 und 2 sowie die Abbildung 1 im von ihr erstellt. Die komplementäre Statistik im „Supplement"-Teil des Manuskripts wurde von Betreuern durchgeführt.

Die gesamte erweiterte Statistik, Tabellen und Abbildungen der Dissertation bzw. des Manteltexts wurden von ihr eigenständig erstellt. Der Erstentwurf hat sie selbstständig formuliert. Danach die Überarbeitung der Veröffentlichung erfolgte mit Unterstützung der Betreuern. Der Manteltext sowie die kritische Interpretation der Arbeit wurden von ihr eigenständig formuliert.

_____
Unterschrift, Datum und Stempel des/der erstbetreuenden Hochschullehrers/in

_____
Unterschrift des Doktoranden/der Doktorandin

VII- Journal summery list

Journal Data Filtered By: **Selected JCR Year: 2018** Selected Editions: SCIE,SSCI
Selected Categories: **"NEUROSCIENCES"** Selected Category Scheme: WoS
Gesamtanzahl: 267 Journale

Rank	Full Journal Title	Total Cites	Journal Impact Factor	Eigenfactor Score
1	NATURE REVIEWS NEUROSCIENCE	43,107	33.162	0.068480
2	NATURE NEUROSCIENCE	63,390	21.126	0.164700
3	ACTA NEUROPATHOLOGICA	20,206	18.174	0.041660
4	BEHAVIORAL AND BRAIN SCIENCES	9,377	17.194	0.010240
5	TRENDS IN COGNITIVE SCIENCES	27,095	16.173	0.040040
6	JOURNAL OF PINEAL RESEARCH	10,695	15.221	0.010560
7	NEURON	95,348	14.403	0.218680
8	TRENDS IN NEUROSCIENCES	20,163	12.314	0.024480
9	Annual Review of Neuroscience	14,042	12.043	0.015020
10	MOLECULAR PSYCHIATRY	20,353	11.973	0.049290
11	BRAIN	52,970	11.814	0.074030
12	BIOLOGICAL PSYCHIATRY	43,122	11.501	0.053320
13	PROGRESS IN NEUROBIOLOGY	12,929	10.658	0.013230
14	Nature Human Behaviour	1,230	10.575	0.006550
15	SLEEP MEDICINE REVIEWS	6,920	10.517	0.010920
16	ANNALS OF NEUROLOGY	37,336	9.496	0.048630
17	Molecular Neurodegeneration	4,248	8.274	0.011350
18	NEUROSCIENCE AND BIOBEHAVIORAL REVIEWS	26,724	8.002	0.051580
19	FRONTIERS IN NEUROENDOCRINOLOGY	4,196	7.852	0.005490
20	Neurology-Neuroimmunology & Neuroinflammation	1,996	7.353	0.008220
21	NEUROPSYCHOPHARMACOLOGY	25,672	7.160	0.039090

Rank	Full Journal Title	Total Cites	Journal Impact Factor	Eigenfactor Score
22	Brain Stimulation	5,457	6.919	0.014470
23	NEUROPATHOLOGY AND APPLIED NEUROBIOLOGY	3,876	6.878	0.006420
24	NEUROENDOCRINOLOGY	5,046	6.804	0.005690
25	NEUROSCIENTIST	4,986	6.791	0.008520
26	BRAIN BEHAVIOR AND IMMUNITY	14,533	6.170	0.025700
27	BRAIN PATHOLOGY	5,263	6.155	0.007880
28	Alzheimers Research & Therapy	3,160	6.142	0.010700
29	JOURNAL OF NEUROSCIENCE	175,046	6.074	0.233460
30	JOURNAL OF CEREBRAL BLOOD FLOW AND METABOLISM	19,766	6.040	0.028050
31	PAIN	38,312	6.029	0.039070
32	CURRENT OPINION IN NEUROBIOLOGY	15,090	6.014	0.033650
33	Acta Neuropathologica Communications	3,063	5.883	0.014190
34	Translational Stroke Research	1,955	5.847	0.004330
35	GLIA	14,003	5.829	0.018760
36	NEUROIMAGE	99,720	5.812	0.132720
37	NEURAL NETWORKS	13,063	5.785	0.016060
38	NEUROPSYCHOLOGY REVIEW	2,971	5.739	0.003940
39	Molecular Autism	2,107	5.712	0.008000
40	Journal of Neuroinflammation	11,767	5.700	0.023240
41	Multiple Sclerosis Journal	11,501	5.649	0.022750
42	Annual Review of Vision Science	458	5.622	0.003300
43	Neurotherapeutics	4,475	5.552	0.009060
44	Translational Neurodegeneration	810	5.534	0.002420

Selected JCR Year: 2018; Selected Categories: "NEUROSCIENCES"

Rank	Full Journal Title	Total Cites	Journal Impact Factor	Eigenfactor Score
45	CEREBRAL CORTEX	30,675	5.437	0.059570
46	JOURNAL OF PAIN	10,405	5.424	0.018280
47	NEUROBIOLOGY OF DISEASE	16,363	5.160	0.026710
48	NEUROINFORMATICS	1,277	5.127	0.002920
49	JOURNAL OF PHYSIOLOGY-LONDON	52,037	4.950	0.041100
50	BIPOLAR DISORDERS	5,143	4.936	0.006760
51	Developmental Cognitive Neuroscience	2,470	4.920	0.009240
52	JOURNAL OF PSYCHIATRY & NEUROSCIENCE	3,293	4.899	0.004540
53	JOURNAL OF NEUROCHEMISTRY	35,902	4.870	0.026140
54	Dialogues in Clinical Neuroscience	3,384	4.867	0.004730
55	Annals of Clinical and Translational Neurology	1,858	4.656	0.008750
56	CURRENT OPINION IN NEUROLOGY	5,290	4.647	0.009650
57	MOLECULAR NEUROBIOLOGY	12,806	4.586	0.027560
58	SLEEP	21,434	4.571	0.024240
59	Current Neuropharmacology	3,508	4.568	0.005650
60	EXPERIMENTAL NEUROLOGY	20,500	4.562	0.023440
61	HUMAN BRAIN MAPPING	22,040	4.554	0.043230
62	Journal of Neural Engineering	7,336	4.551	0.012190
63	EUROPEAN NEUROPSYCHOPHARMACOLOGY	7,488	4.468	0.015500
64	CEPHALALGIA	9,983	4.438	0.014480
65	NEUROBIOLOGY OF AGING	22,409	4.398	0.037090
66	EUROPEAN JOURNAL OF NEUROLOGY	10,488	4.387	0.016970

Selected JCR Year: 2018; Selected Categories: "NEUROSCIENCES"

Rank	Full Journal Title	Total Cites	Journal Impact Factor	Eigenfactor Score
67	NEUROPHARMACOLOGY	20,604	4.367	0.034460
68	PROGRESS IN NEURO-PSYCHOPHARMACOLOGY & BIOLOGICAL PSYCHIATRY	10,674	4.315	0.012400
69	Cognitive Computation	1,578	4.287	0.002230
70	CORTEX	10,302	4.275	0.024590
71	Neuroscience Bulletin	2,027	4.246	0.004070
72	JOURNAL OF PSYCHOPHARMACOLOGY	6,460	4.221	0.010120
73	INTERNATIONAL JOURNAL OF NEUROPSYCHOPHARMACOLOGY	6,551	4.207	0.012320
74	JOURNAL OF NEUROSCIENCE RESEARCH	12,976	4.139	0.010060
75	Molecular Brain	2,467	4.051	0.007180
76	PSYCHONEUROENDOCRINOLOGY	16,809	4.013	0.028150
77	NEUROCHEMISTRY INTERNATIONAL	8,775	3.994	0.009020
78	NUTRITIONAL NEUROSCIENCE	1,778	3.950	0.002260
79	Frontiers in Systems Neuroscience	4,801	3.928	0.015360
80	JOURNAL OF HEADACHE AND PAIN	3,308	3.918	0.007210
81	Frontiers in Cellular Neuroscience	9,711	3.900	0.035870
82	Journal of Neuroimmune Pharmacology	2,486	3.870	0.004750
83	ACS Chemical Neuroscience	5,238	3.861	0.013320
84	CELLULAR AND MOLECULAR NEUROBIOLOGY	4,488	3.811	0.005740
85	NEUROGASTROENTEROLOGY AND MOTILITY	8,314	3.803	0.014510
86	JOURNAL OF NEUROTRAUMA	14,754	3.754	0.019770
87	Fluids and Barriers of the CNS	1,127	3.727	0.002650
88	Frontiers in Molecular Neuroscience	4,752	3.720	0.014230

Selected JCR Year: 2018; Selected Categories: "NEUROSCIENCES"

Rank	Full Journal Title	Total Cites	Journal Impact Factor	Eigenfactor Score
89	Journal of Parkinsons Disease	1,768	3.698	0.006340
90	CLINICAL NEUROPHYSIOLOGY	19,574	3.675	0.021420
91	Social Cognitive and Affective Neuroscience	6,966	3.662	0.020880
92	Frontiers in Neuroscience	13,198	3.648	0.043000
93	Frontiers in Aging Neuroscience	6,791	3.633	0.020910
94	Brain Structure & Function	6,077	3.622	0.019520
95	NEURAL PLASTICITY	3,691	3.591	0.010510
96	Journal of Neurodevelopmental Disorders	1,253	3.590	0.003420
97	Journal of NeuroEngineering and Rehabilitation	4,974	3.582	0.008800
98	Neurophotonics	809	3.581	0.002760
99	JOURNAL OF ALZHEIMERS DISEASE	20,383	3.517	0.041470
100	PSYCHIATRY AND CLINICAL NEUROSCIENCES	3,720	3.489	0.004230
101	JOURNAL OF NEUROPATHOLOGY AND EXPERIMENTAL NEUROLOGY	9,205	3.460	0.007510
102	JOURNAL OF SLEEP RESEARCH	5,432	3.432	0.007450
103	PSYCHOPHARMACOLOGY	23,565	3.424	0.022260
104	Current Opinion in Behavioral Sciences	1,763	3.422	0.009020
105	CEREBELLUM	2,785	3.413	0.005970
106	Current Neurology and Neuroscience Reports	3,004	3.400	0.007210
107	CNS Neuroscience & Therapeutics	2,993	3.394	0.005990
108	PSYCHOPHYSIOLOGY	14,275	3.378	0.012150
109	Cognitive Neuroscience	570	3.361	0.001630
110	NEUROTOXICITY RESEARCH	3,067	3.311	0.003750

Selected JCR Year: 2018; Selected Categories: "NEUROSCIENCES"

VIII- Publication

https://doi.org/10.3233/JAD-200520

IX- Curriculum Vitae

Mein Lebenslauf wird aus datenschutzrechtlichen Gründen in der elektronischen Version meiner Arbeit nicht veröffentlicht.

Mein Lebenslauf wird aus datenschutzrechtlichen Gründen in der elektronischen Version meiner Arbeit nicht veröffentlicht.

X- Publication list

Selected journal articles:

1) Sen, A., **Hallab, A**., Cross, J. H., Sander, J. W., & Newton, C. R. (2021). Optimising epilepsy care throughout the Afghan refugee crisis. Lancet (London, England), 398(10311), 1563. (**IF= 202.731**)

2) Hallab, A., & Sen, A. (2021). Epilepsy and psychogenic non-epileptic seizures in forcibly displaced people: A scoping review. Seizure, 92, 128–148. (**IF= 3.414**)

3) Andraus, M., Thorpe, J., Tai, X. Y., Ashby, S., **Hallab, A.,** Ding, D., Dugan, P., Perucca, P., Costello, D., French, J. A., O'Brien, T. J., Depondt, C., Andrade, D. M., Sengupta, R., Delanty, N., Jette, N., Newton, C. R., Brodie, M. J., Devinsky, O., Helen Cross, J., Sander, J. W., Jane, H., Sen, A., COVID-19, Epilepsy COV-E Study Group (2021). Impact of the COVID-19 pandemic on people with epilepsy: Findings from the Brazilian arm of the COV-E study. Epilepsy & behavior : E&B, 123, 108261. (**IF= 3.337**)

4) Thorpe, J., Ashby, S., **Hallab, A.,** Ding, D., Andraus, M., Dugan, P., Perucca, P., Costello, D., French, J. A., O'Brien, T. J., Depondt, C., Andrade, D. M., Sengupta, R., Delanty, N., Jette, N., Newton, C. R., Brodie, M. J., Devinsky, O., Helen Cross, J., Sander, J. W., Jane, H., Sen, A., COVID-19 and Epilepsy (COV-E) Study Group (2021). Evaluating risk to people with epilepsy during the COVID-19 pandemic: Preliminary findings from the COV-E study. Epilepsy & behavior : E&B, 115, 107658. (**IF= 3.337**)

5) Hallab, A., Lange, C., Apostolova, I., Özden, C., Gonzalez-Escamilla, G., Klutmann, S., Brenner, W., Grothe, M. J., Buchert, R., & Alzheimer's Disease Neuroimaging Initiative (2020). Impairment of Everyday Spatial Navigation Abilities in Mild Cognitive Impairment Is Weakly Associated with Reduced Grey Matter Volume in the Medial Part of the Entorhinal Cortex. Journal of Alzheimer's disease : JAD, 78(3), 1149–1159. (**IF=4.472 for 2020**)

6) Hallab, A., Naveed, S., Altibi, A., Abdelkhalek, M., Ngo, H. T., Le, T. P., Hirayama, K., & Huy, N. T. (2018). Association of psychosis with antiphospholipid antibody syndrome: A systematic review of clinical studies. General hospital psychiatry, 50, 137–147. (**IF=3.220 for 2018**)

7) Morra, M. E., Altibi, A., Iqtadar, S., Minh, L., Elawady, S. S., **Hallab, A**., Elshafay, A., Omer, O. A., Iraqi, A., Adhikari, P., Labib, J. H., Elhusseiny, K. M., Elgebaly, A., Yacoub, S., Huong, L., Hirayama, K., & Huy, N. T. (2018). Definitions for warning signs and signs of severe dengue according to the WHO 2009 classification: Systematic review of literature. Reviews in medical virology, 28(4), e1979. (**IF=4.221 for 2018**)

XI- Acknowledgment

First, I would like to express my sincere gratitude and appreciation for my supervisor

Prof. Dr. med. W. Brenner

whose guidance, support and encouragement have been of high value throughout this work. His thoughtful comments and recommendations have made this dissertation an inspiring experience for me and encouraged me in all the time of my academic research.

Furthermore, I am very thankful to my supervisor

Dr. rer. nat. R. Buchert

for guiding and assisting me at every stage of the dissertation project. His overall insights and knowledge into the field steered me through this dissertation.

My appreciation also goes out to my family and friends for their encouragement and support.